Sb-based infrared detectors and FPAs at JPL

Alexander Soibel, David Z.-Y. Ting, Sir. B. Rafol, Arezou Khoshakhlagh, Cpry Hill, Linda Hoglund, Anita Fisher, Sam. A. Keo, and Sarath D. Gunapala

Infrared Photonics Group
Jet Propulsion Laboratory
California Institute of Technology

© 2016 California Institute of Technology. Government sponsorship acknowledged

Infrared FPAs for Space Applications……

One of the interests of NASA is to map the sky in high resolution infrared instrument such as , Wide-field infrared survey explorer (WISE), Spitzer Telescope, and Keppler. They especially look for:

- Brown dwarfs (cool stars)
- Asteroids
- Neighboring galaxies
- Proto-stars
- Earth like planets at the edge of Orion arm

Visible light

Infrared light

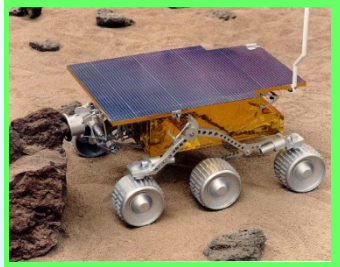

Pathfinder

Spirit & Opportunity

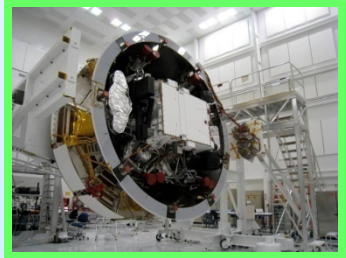

Mars Science Laboratory

1. Mariner I (1977)
2. Mariner II (1977)
3. Mars Observer (1992)
4. Mars Pathfinder (1997)
5. Mars Global Surveyor (1999)
6. Mars Climate Orbiter (2001)
7. Mars Polar Lander (2001)
8. Mars Odyssey (2003)
9. Spirit & Opportunity (2005)
10. Mars Reconnaissance Orbiter (2005)
11. Phoenix Lander (2008)
12. Mars Science Laboratory (2011)
13. Mars 2018

Super Earth's near in our neighborhood

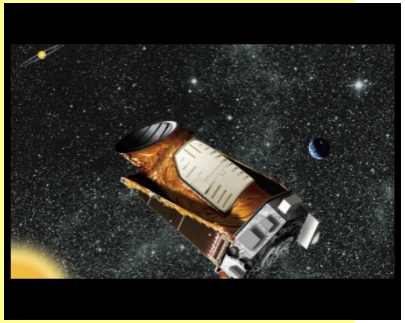

Keppler looking for Earth like planets in Orion arm

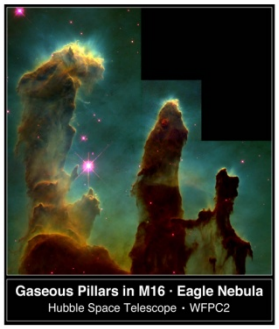

New born proto-stars in Eagle nebula

Mar missions study mineral, water, methane, etc. Mars missions require 0.4 – 4 μm high performance arrays operating at high operating temperatures (passive cooling).

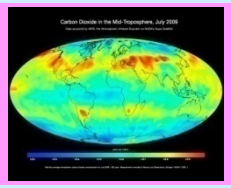

NASA also monitors the infrared spectrum in the earth atmosphere as a function of height with Atmospheric Infrared Sounder (AIRS). This gives information about temperature and trace components in the atmosphere such as ozone, CO_2 and methane.

Outline

- **Quantum Well Infrared Detectors**

- Antimonide-based superlattice (SL) infrared photodetectors

- Barrier Infrared Detector (BIRD)
  - Complementary Barrier Infrared Detector (CBIRD)
  - CBIRD focal plane array
  - InAsSb barrier detectors
  - Quantum Dot Barrier Infrared detectors

- Ga-free InAs/InAsSb superlattices

QWIP: structure, growth and light coupling

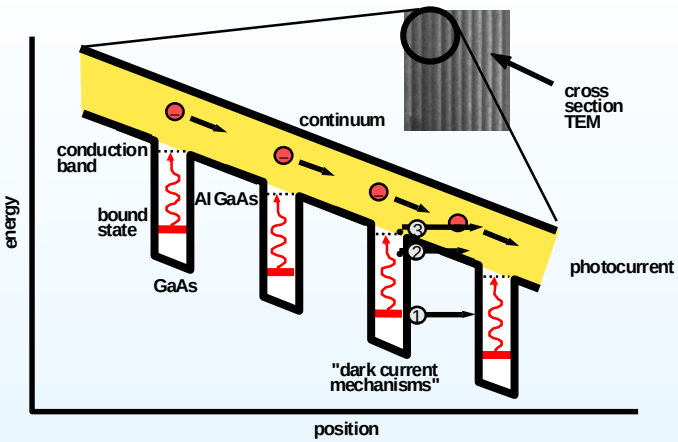

QWIP Band Diagram

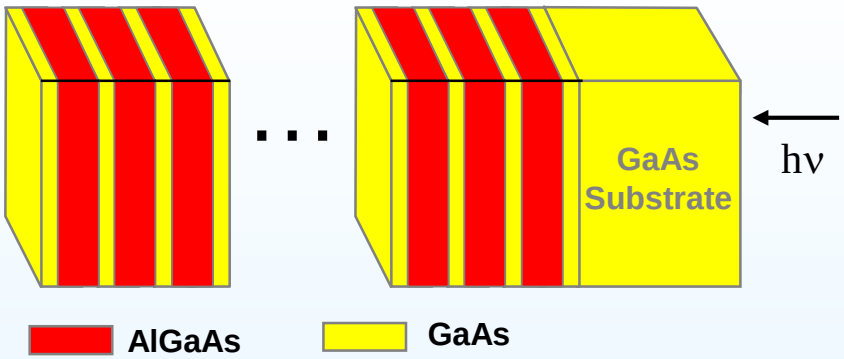

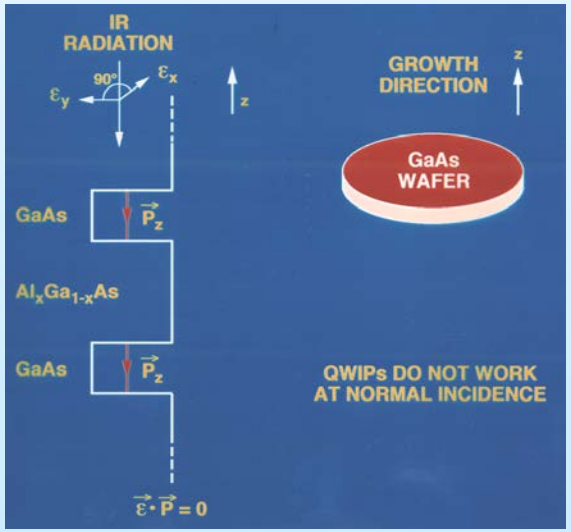

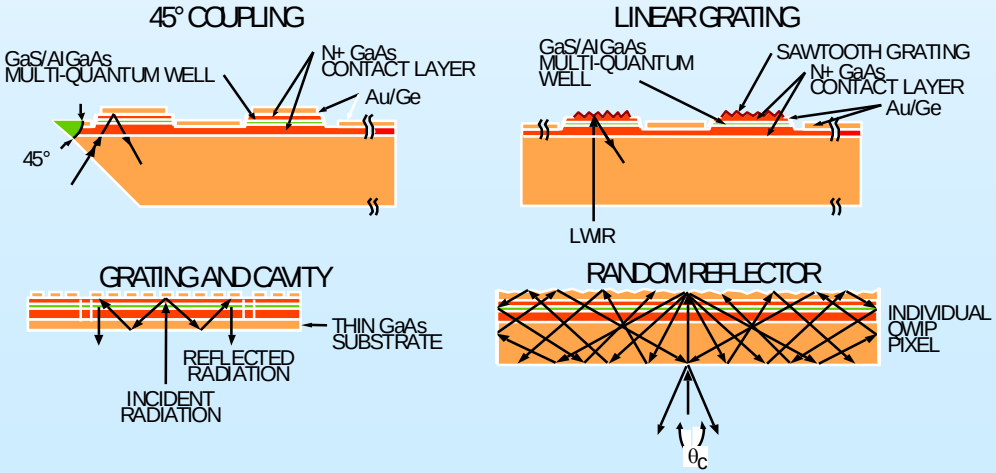

Focal Plane Array Fabrication Process

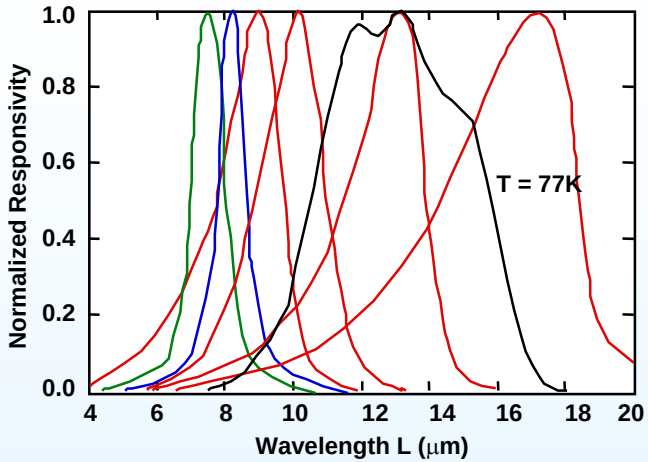

GaAs/AlGaAs Based QWIP Can Cover a Very Broad Infrared (3-25 μm) Region

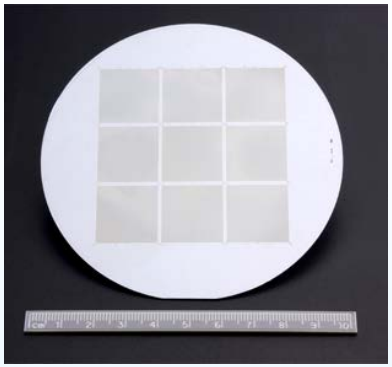

Nine 1024 x 1024 QWIP Focal Plane Arrays (FPAs) on 4-inch GaAs Wafer

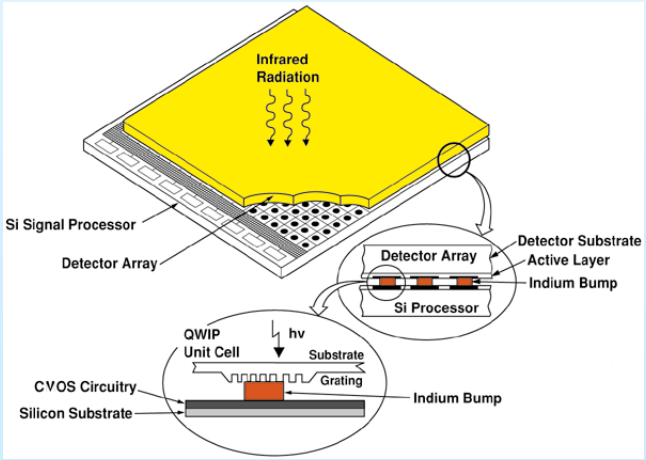

Indium Bump Bonding Process

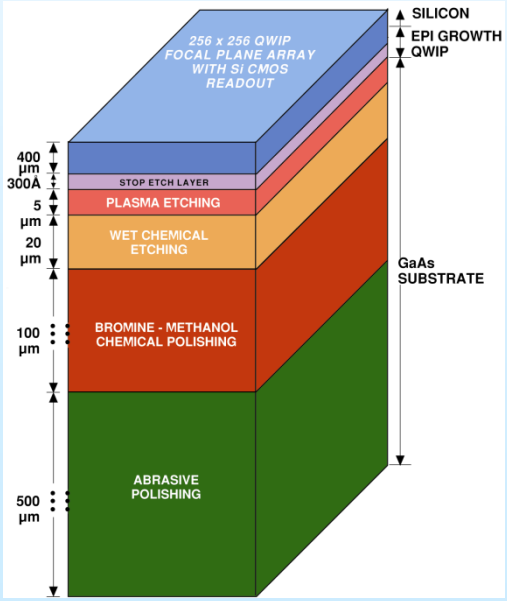

FPA Thinning Process

Broadband QWIP

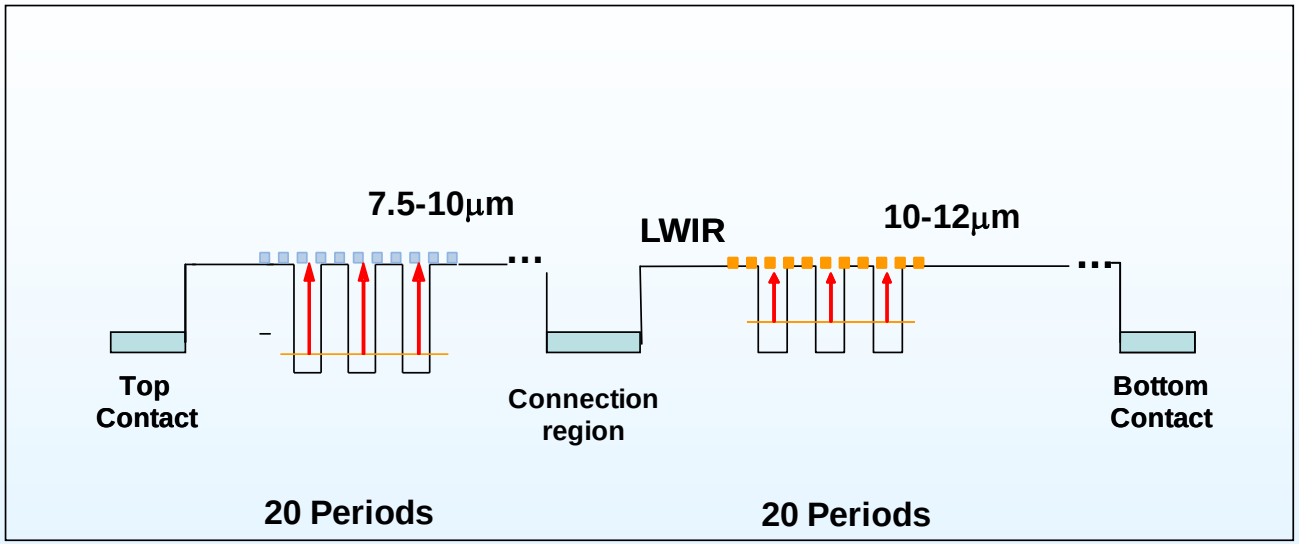

- QWIP is based on a resonant absorption between ground state and a quasi-continuum state
- The spectral response of QWIPs are inherently narrow-band and the typical full-width at half-maximum (FWHM) is about 10% of the peak wavelength
- The spectrometer requires infrared sensor with <u>broad spectral coverage therefore multi-wavelength or broadband QWIP need to be used in this application</u>

-In these QWIPs multi-quantum well (MQW) stacks are vertical integrated. Each MQW stack absorbs photons within the specified wavelength band allowing other photons to pass through

- Two color stack is used in HyTES QWIP

FPA Fabrication

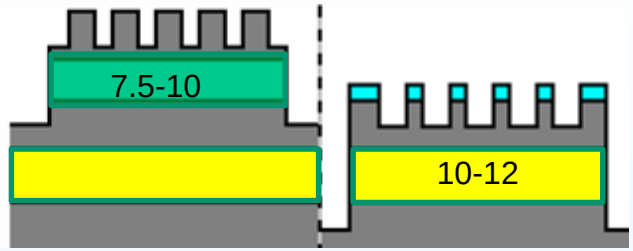

HyTES pixel design – cross-sectional zoom at the transition point, showing two bands with ¼ lambda gratings on each

Map of FPA grating regions. The target spectral band of each grating region is indicated in the map.

Image acquired with developed 1024x1024 QWIP FPA operating at *T* = 40 K with a frame rate of 15 Hz, integration time of 9 msec, and f/2 cold stop

Two point Corrected Image

Hyperspectral Thermal Emission Spectrometer (HyTES) First Flights

Jet Propulsion Laboratory
California Institute of Technology

Left: Cuprite, NV 2012-07-20, bands 150 (10.08 µm), 100 (9.17 µm), 58 (8.41 µm) displayed as RGB respectively as image cube.

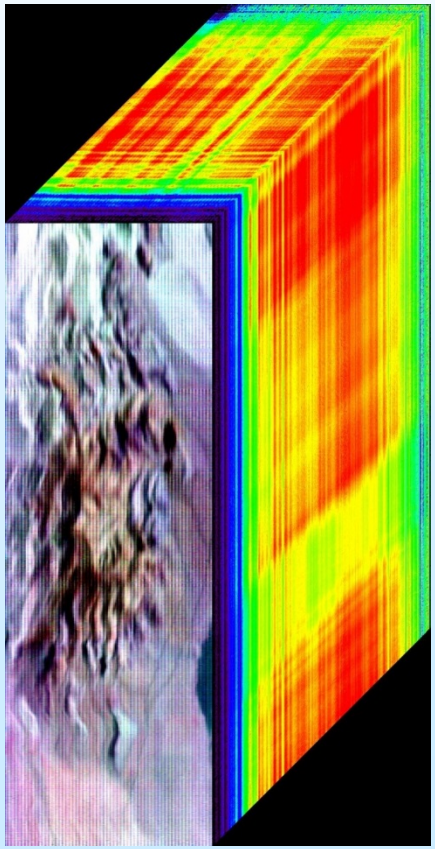

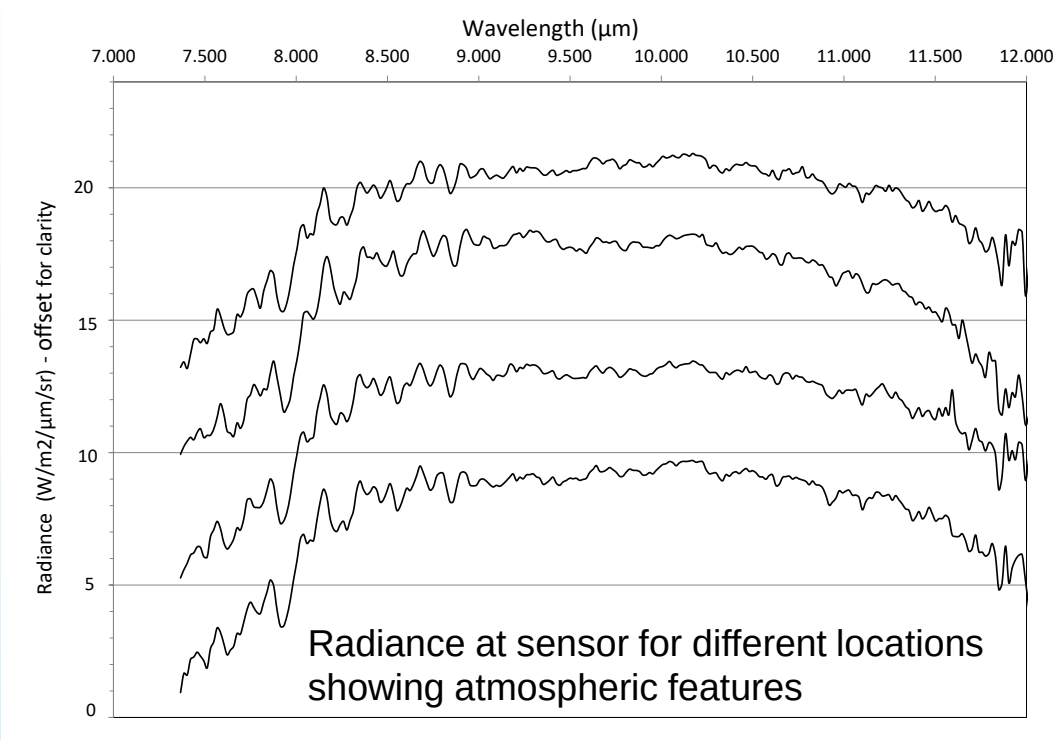

Noise Equivalent Delta Temperature (NEdT) ~0.2K

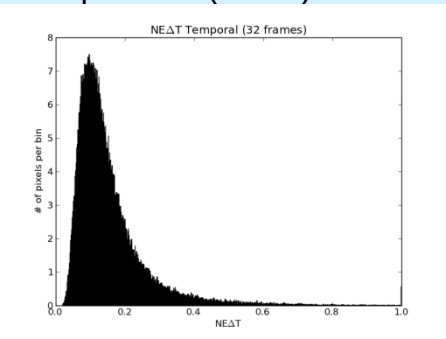

Blackbody Cross track uniformity

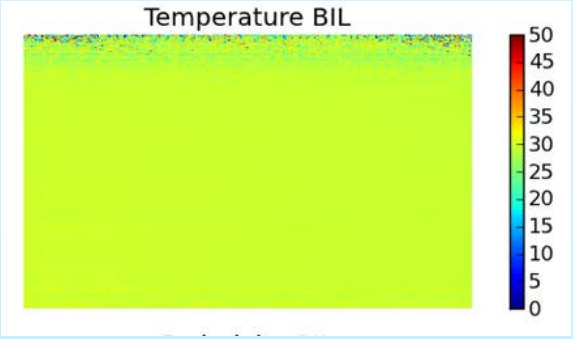

Outline

- Quantum Well Infrared Detectors
- **Antimonide-based superlattice (SL) infrared photodetectors**
- Barrier Infrared Detector (BIRD)
  - Complementary Barrier Infrared Detector (CBIRD)
  - CBIRD focal plane array
  - InAsSb barrier detectors
  - Quantum Dot Barrier Infrared detectors
- Ga-free InAs/InAsSb superlattices

Material Robustness

Semiconductor Families for Infrared Photodetection

	Si	Ge	GaAs	AlAs	InP	InGaAs	AlInAs	InAs	GaSb	AlSb	InSb	HgTe	CdTe
Group	IV	IV	III-V	III-V	III-V	III-V	III-V	III-V	III-V	III-V	III-V	II-VI	II-VI
Lattice Constant [Å]	5.431	5.658	5.653	5.661	5.870	5.870	5.870	6.058	6.096	6.136	6.479	6.453	6.476
Bulk Modulus [Gpa]	98	75	75	74	71	69	66	58	56	55	47	43	42
Direct Gap [eV] (λ [μm])	-	-	1.426 (0.87)	-	1.350 (0.92)	0.735 (1.69)	-	0.354 (3.5)	0.730 (1.7)	-	0.175 (7.1)	-0.141	1.475
MWIR/ LWIR Detection Mechanism	Heterojunction Internal photoemission (HIP)		Quantum well/dot Intersubband (QWIP/ QDIP)		Quantum well Intersubband (QWIP)			Bulk (MW) / Superlattice (MW/LW) Band-to-Band			Bulk B-B	Bulk Band-to-Band	

General Trends

Larger lattice constant

Weaker chemical bond (less covalent / more ionic)

Decreasing material robustness / manufacturability

Smaller band gap (enables strong band-to-band IR absorption)

Higher quantum efficiency

Antimonides Material System for Type-II Superlattices

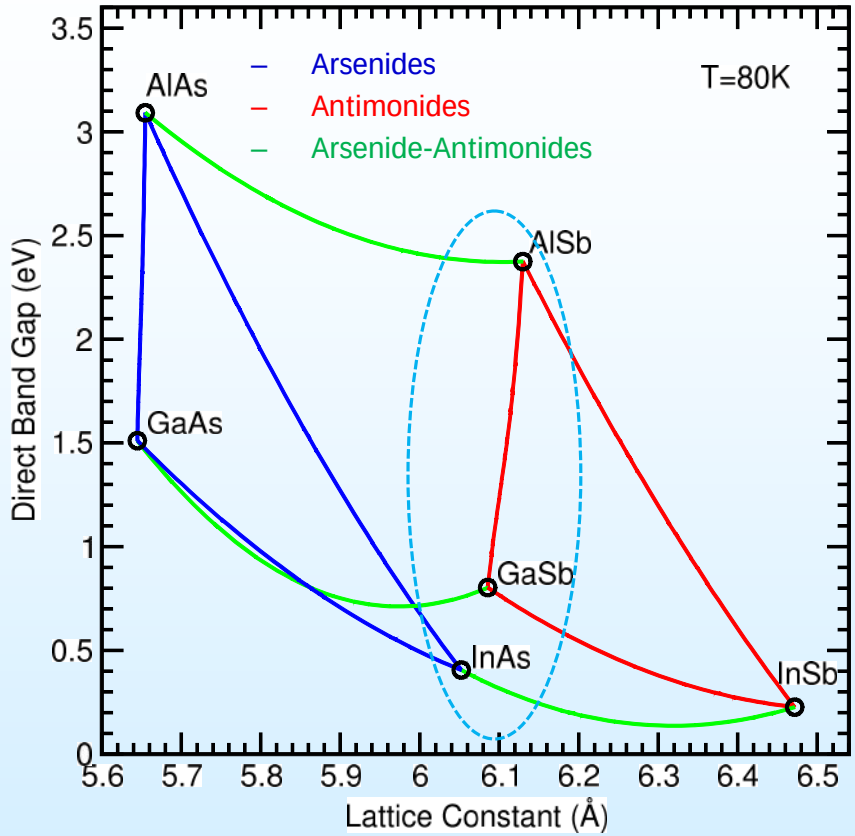

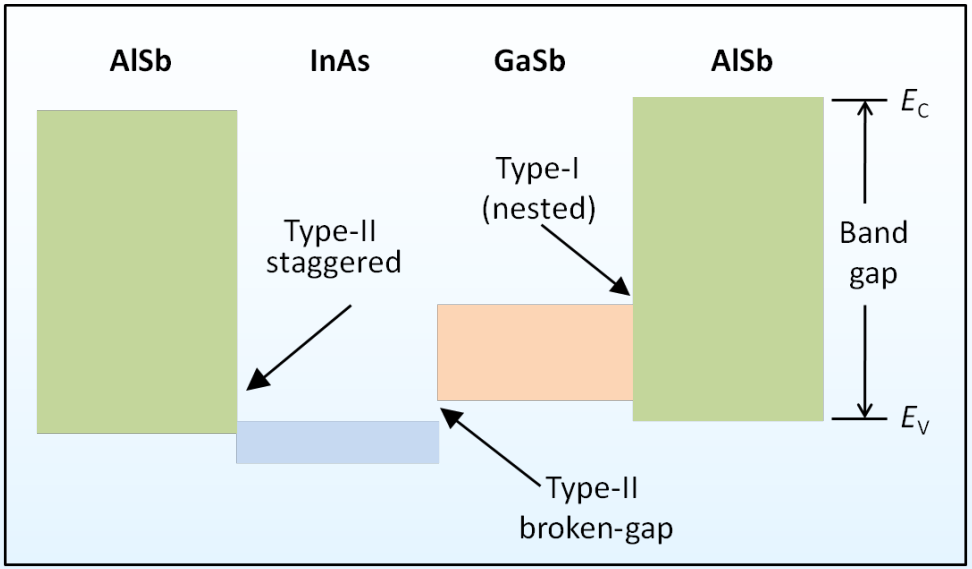

- Material system includes InAs, GaSb, AlSb and their alloys
  - Nearly lattice matched (~6.1 Å)
- Alloys with GaAs, AlAs, and InSb adds even more flexibility

- Three types of band alignments
  - Type-I (nested, straddling)
  - Type-II staggered
  - Type-II broken gap (misaligned, Type-III)
    - Unique among common semiconductor families
    - Overlap between InAs CB and GaSb VB enables interband devices
- Tremendous flexibility in artificially designed materials / device structures

Basic Properties of InAs/Ga(In)Sb Type-II Superlattice

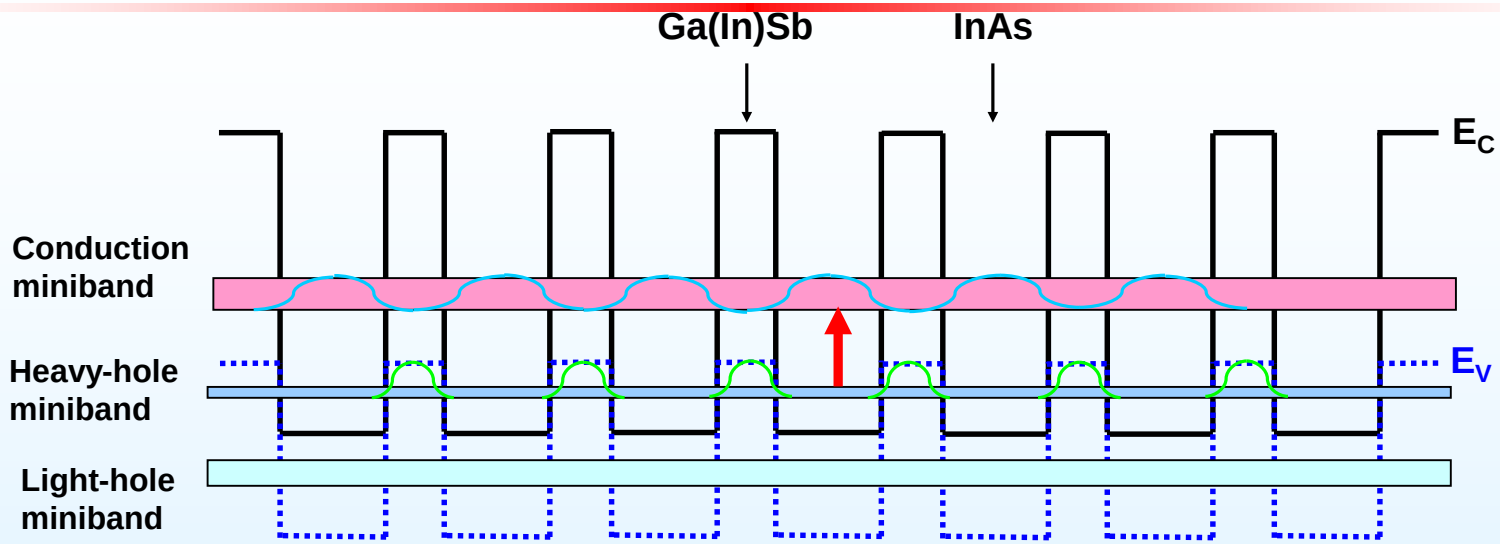

- Type-II broken-gap superlattice
  - Spatially separated CB and VB wave functions
    - Reduced oscillator strength (compensated by larger VB edge density of states)
  - Type-II SL band gap smaller than gap of either bulk semiconductors
    - Type-I SL band gap always larger than the smaller bulk gap
  - Nearly independent control of conduction and valence subband edges
    - Important for manipulating band alignments

Key Properties of Type-II Superlattices

- Infrared band gap
  - SWIR to VLWIR
- Absorption strength comparable to MCT

Advantages:

- Lower tunneling leakage
- Reduced diffusion dark current (p-type)
- Reduced Auger generation

Challenges:

- G-R dark current induced by SRH processes
- Lifetime significantly lower than MCT
  - Attributed to SRH
  - Effect of short lifetime on diffusion dark current ?
- Surface leakage

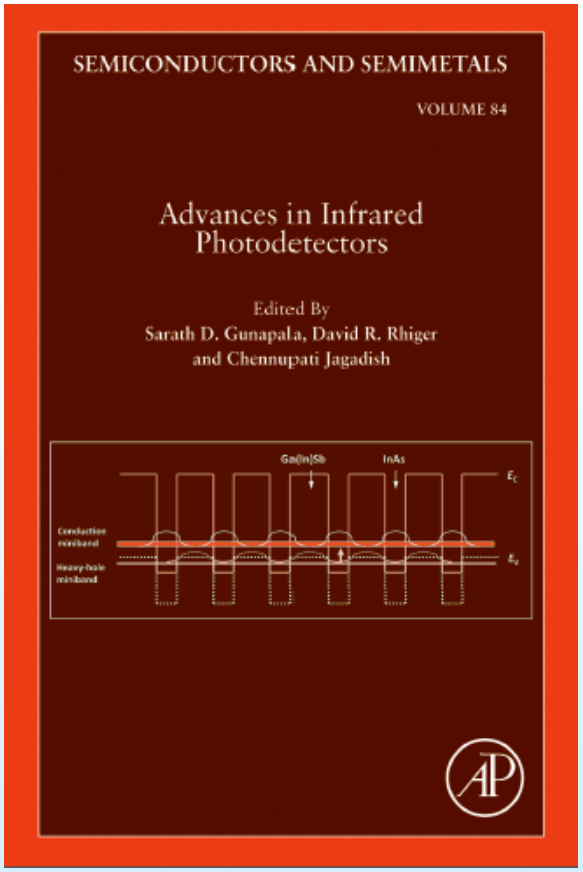

"Type-II Superlattice Infrared Detectors", *D. Z. Ting, A. Soibel, L. Höglund, J. Nguyen, C. J. Hill, A. Khoshakhlagh, and S. D. Gunapala, Semiconductors and Semimetals* **84**, pp.1-57 (2011).

G-R Dark Current Suppression using Unipolar Barriers

Dark Current Mechanisms in a Homojunction Diode

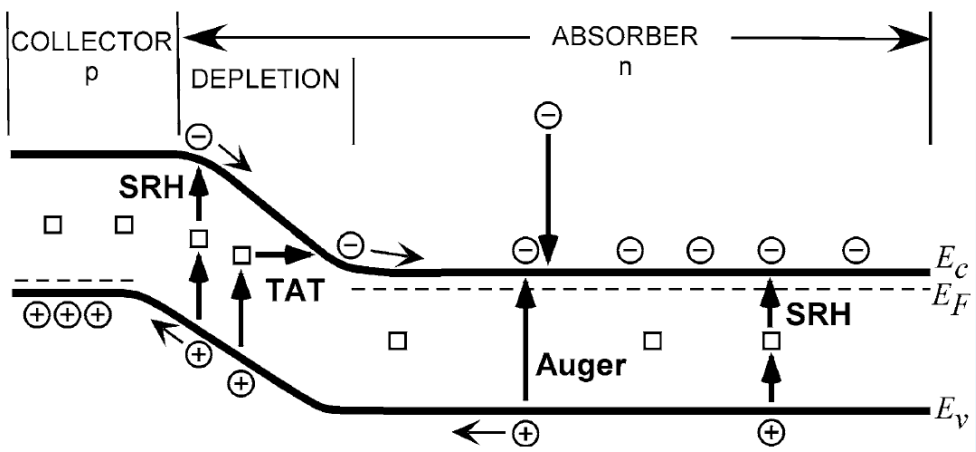

D. R. Rhiger, J. Electronic Materials, 40(8) 1815 (2011)

- High performance IR detector requires good signal (photoresponse; QE) to noise (dark current) ratio
  - High QE achieved using thick, strain-balanced absorbers
- Dark current mechanisms in a p-on-n homojunction
  - Trap assisted tunneling, band-to-band tunneling
  - G-R current from SRH processes in depletion region
  - Diffusion dark current from Auger and SRH processes in quasi-neutral region
  - Surface leakage current (not shown)
- Designs based on heterostructures can enhance performance

Unipolar Barriers

Electron blocking barrier

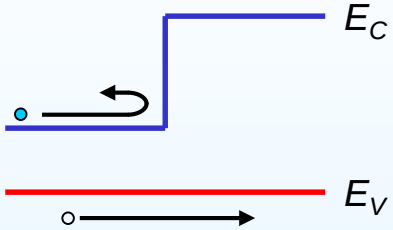

Hole blocking barrier

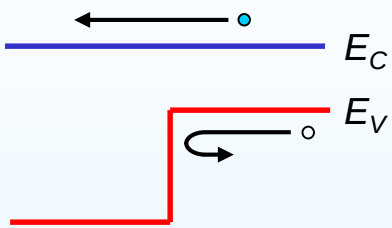

- Unipolar barriers:
  - Block one carrier type, but allows un-impeded flow of the other
  - Electron barrier
  - Hole barrier
  - Terminology introduced in Ting et al. *Appl. Phys. Lett.* **95**, 023508 (2009), now in common usage

Double Heterostructure Laser

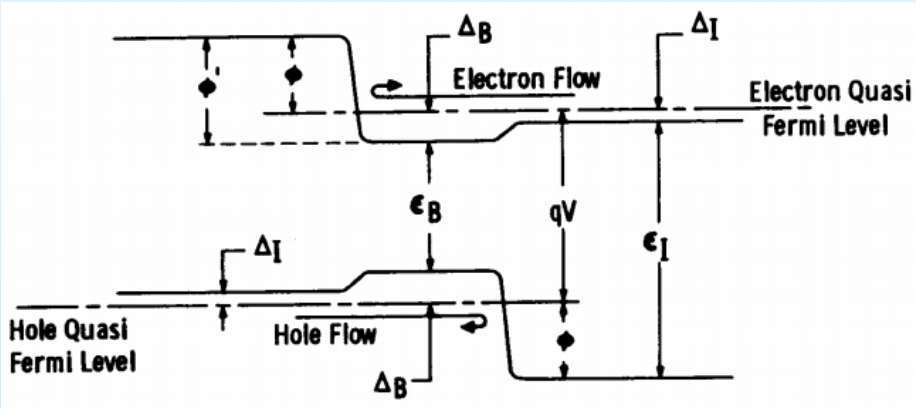

- Using unipolar barriers to enhance semiconductor device performance
  - DH Laser, H. Kroemer, Proc. IEEE 1963
  - DH Laser, Zh. I. Alferov and R. F. Kazarinov, patent certificate (Russian) 1963

Copyright 2011. All rights reserved.

SRH Suppression in LWIR SL Heterodiode

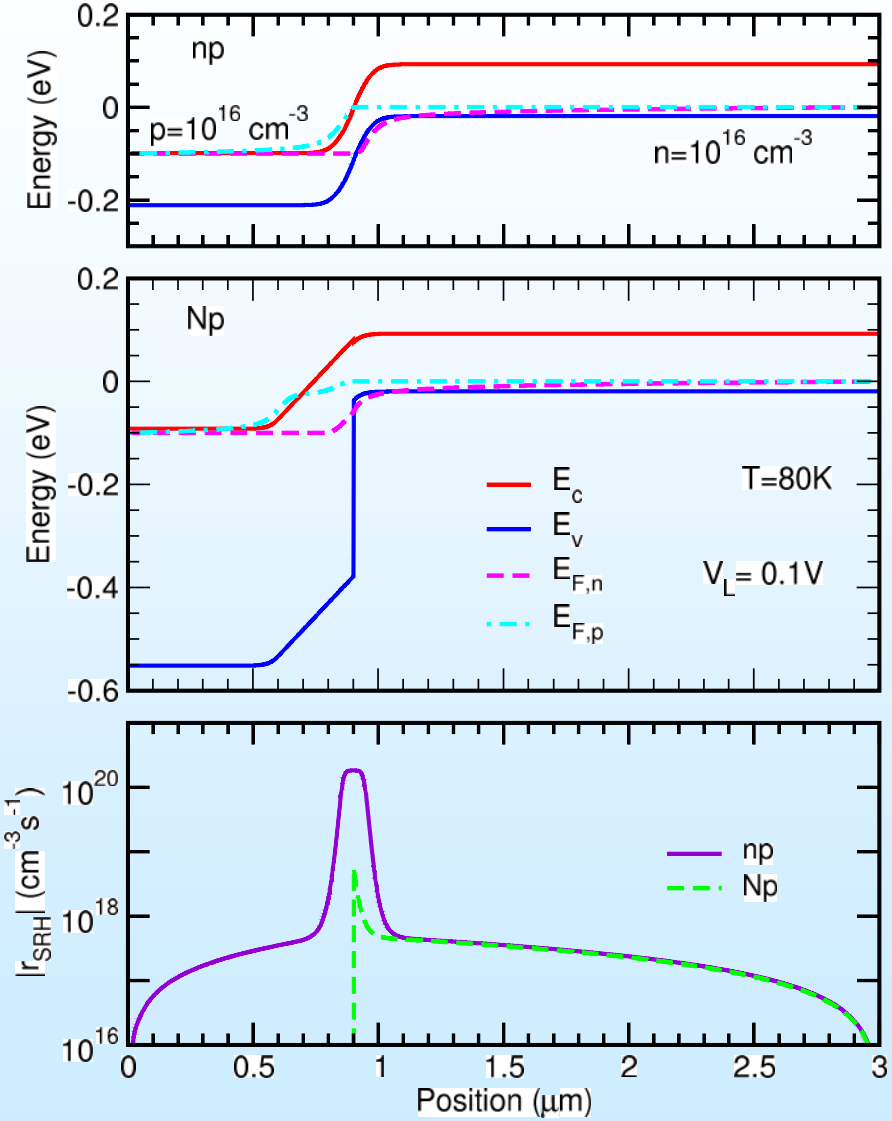

- Drift-diffusion simulation comparing LWIR SL np and Np diodes
- np homodiode
  - LWIR InAs/GaSb SL
- Np heterodiode
  - LWIR InAs/AlSb SL p-type absorber
  - InAs/AlSb SL hole-blocking unipolar barrier
  - Hole barrier does not block photocurrent
- SRH recombination rate given by

$$r_{SRH} = (np - n_i^2) / [(\tau_p (n + n_i) + (\tau_n (p + p_i)]$$

- The Np heterostructure can be effective at SRH suppression

Outline

- Quantum Well Infrared Detectors
- Antimonide-based superlattice (SL) infrared photodetectors
- Barrier Infrared Detector (BIRD)
  - **Complementary Barrier Infrared Detector (CBIRD)**
  - CBIRD focal plane array
  - InAsSb barrier detectors
  - Quantum Dot Barrier Infrared detectors
- Ga-free InAs/InAsSb superlattices

CBIRD Structure

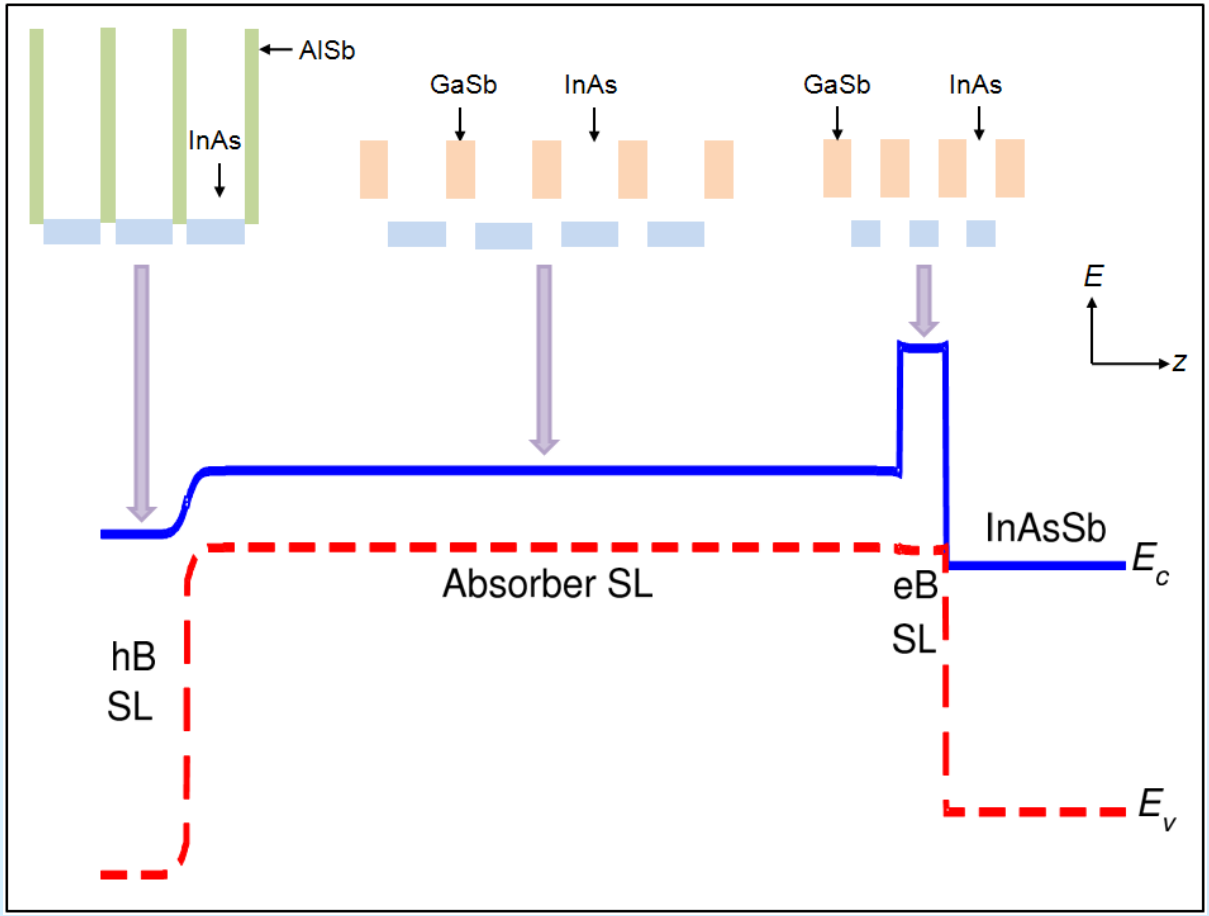

- Complementary Barrier Infrared Detector (CBIRD)
- p-type LWIR superlattice absorber surrounded by
  - n-doped unipolar hole barrier (hB)
  - p-doped unipolar electron barrier (eB)
- Bottom tunneling contact

CBIRD Characteristics

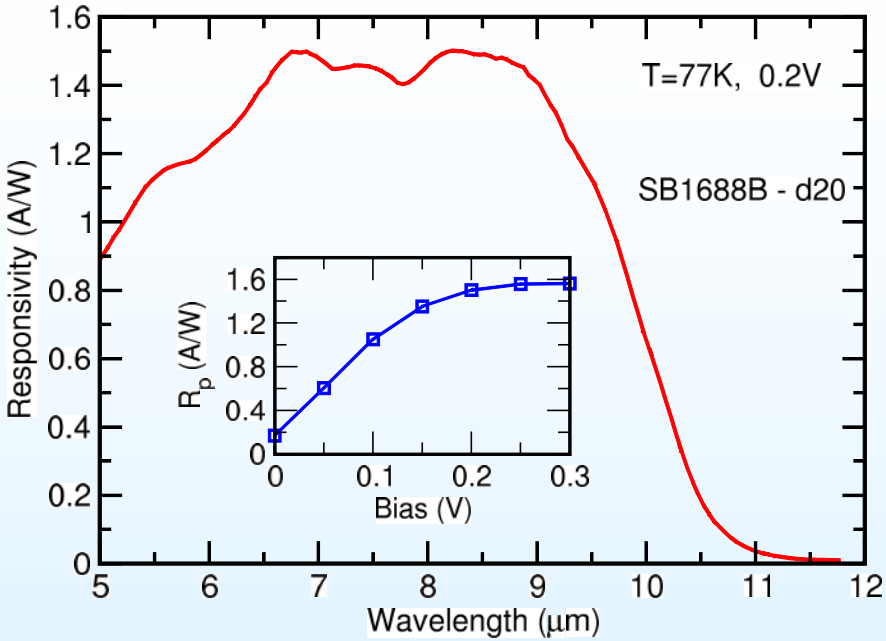

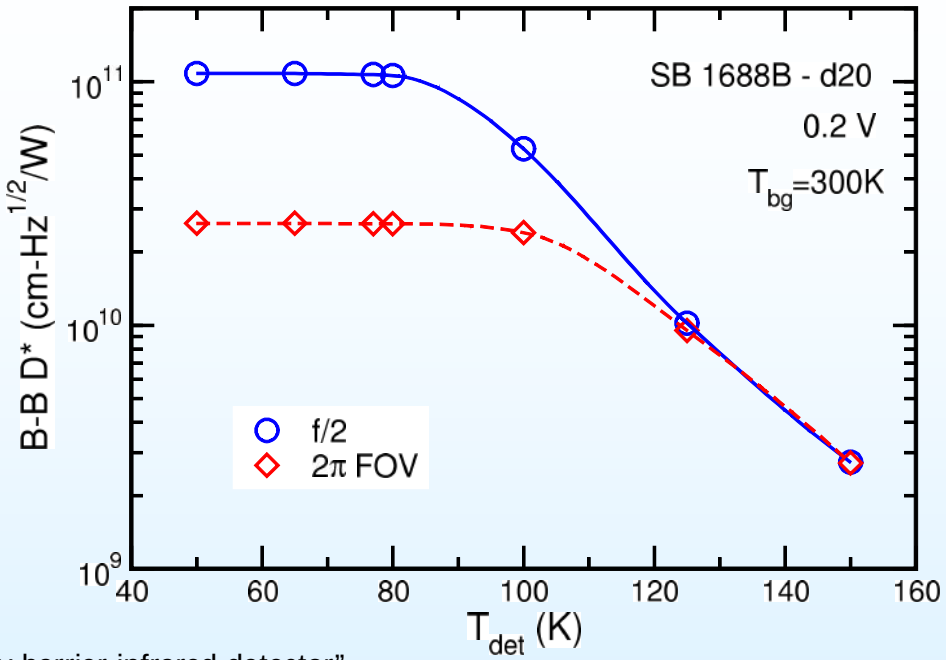

"A high-performance long wavelength superlattice complementary barrier infrared detector",
D. Z.-Y. Ting, C. J. Hill, A. Soibel, S. A. Keo, J. M. Mumolo, J. Nguyen, S. D. Gunapala, *Appl. Phys. Lett.* **95**, 023508 (2009).

- Discrete 220 μm × 220 μm devices
- 10 μm cutoff (50% peak responsivity)
- R_{peak} = 1.5 A/W at 0.2 V (λ_p=8.2 μm);
  - QE=27% (single pass, no AR coating)
- J_d(0.2V, 77K) = 1x10^{-5} A/cm^2
- Black-body D* (8 μm to 10 μm; 300K background), f/2 optics:
  - T_{BLIP}= 86K, (BLIP condition: I_{dark} < ¼ I_{photo})
  - B-B BLIP *D** = 1.1×10^{11} cm-Hz$^{1/2}$/W

CBIRD with Zero Turn-On Bias

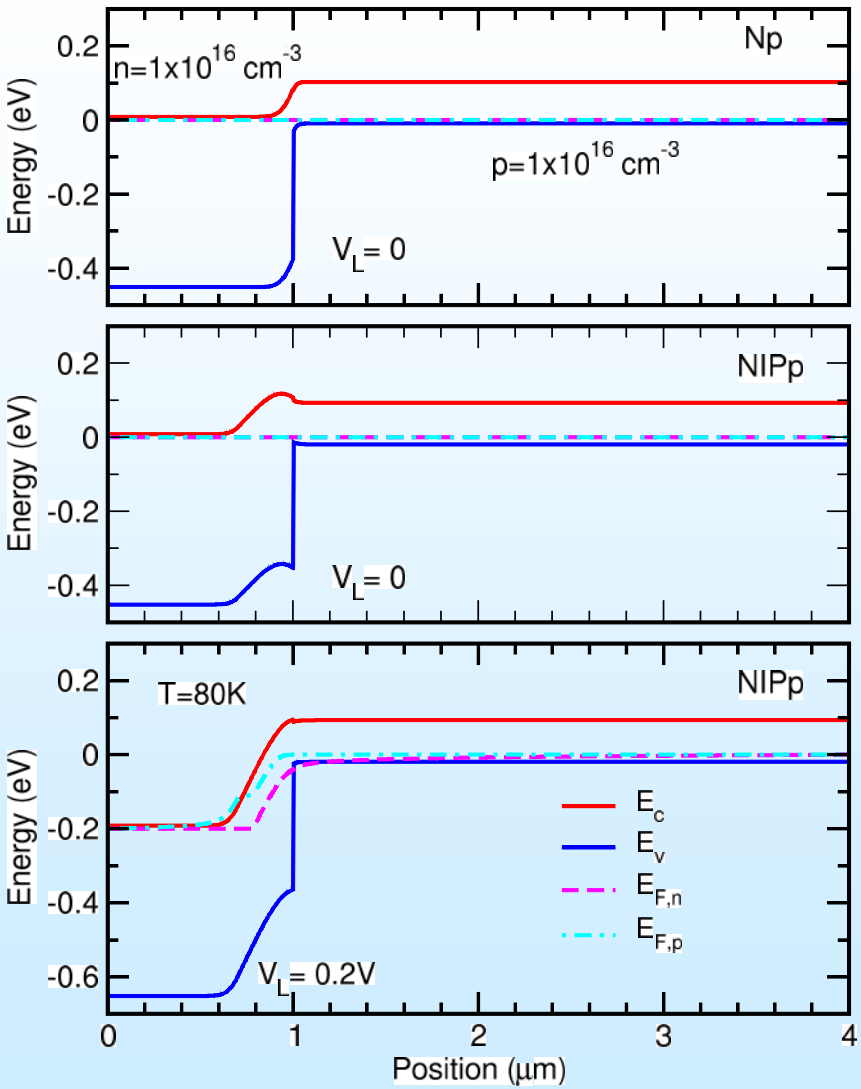

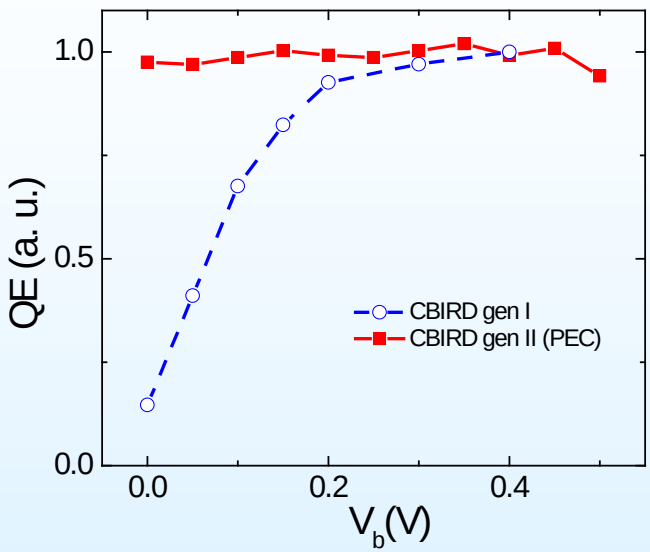

- The 200 mV turn-on bias in original CBIRD device attributed to un-intended electron barrier at the hole-barrier/ absorber interface
- Attributed to unintended conduction band offset or dopant migration (see figure at left)
- New CBIRDs turn on at zero bias

Noise Measurement: Frequency and Bias Dependence

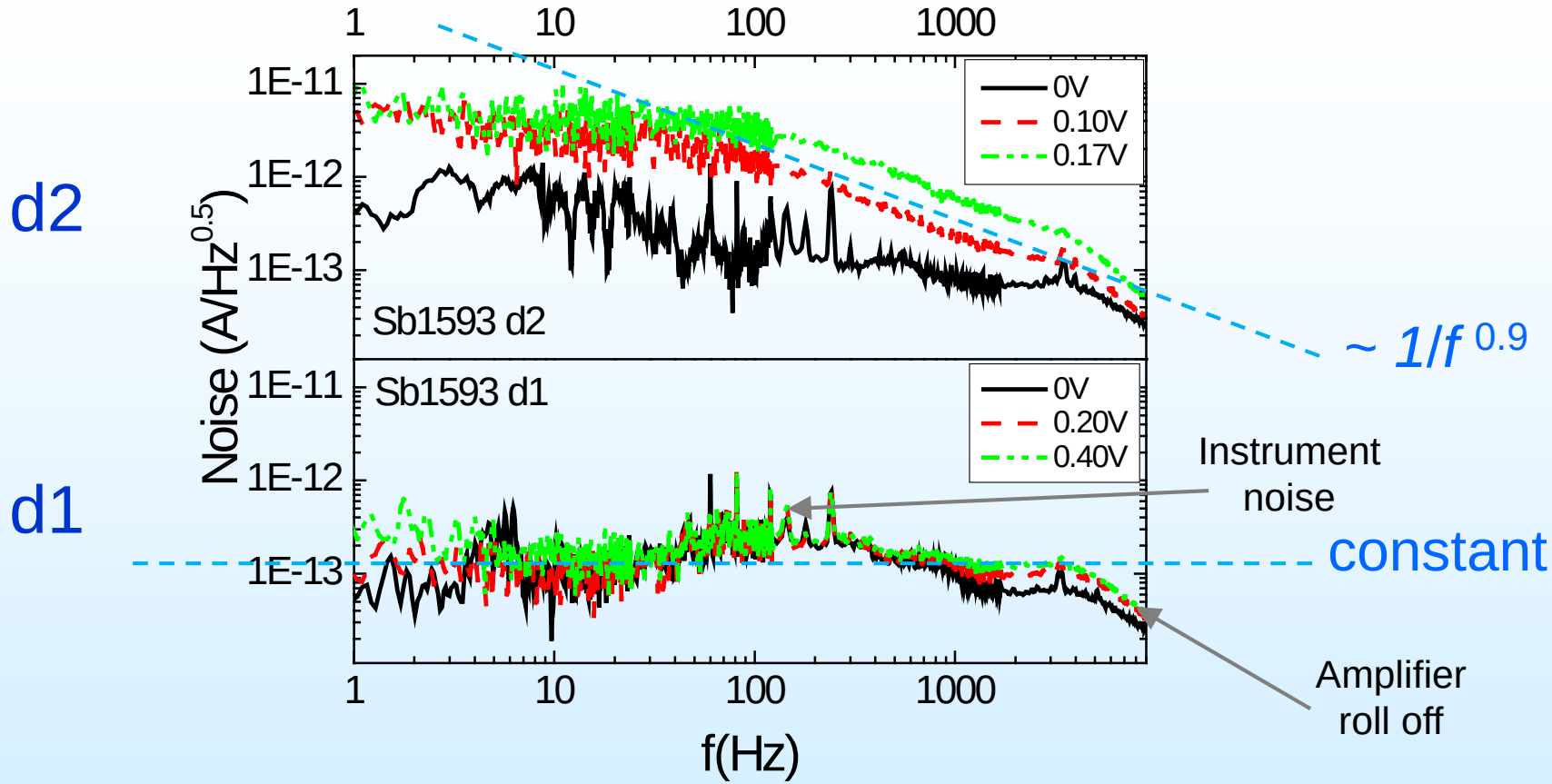

- Superlattice photodetectors studied exhibit no intrinsic (bulk) high 1/f noise
- Measurements clearly show that sidewall leakage current contributes to:
  - increased shot noise (from higher dark current)
  - also additional frequency dependent noise

Appl. Phy. Lett. **96**(11), 111102 (2010).

Optical studies of InAs/GaSb superlattices

We performed optical studies of InAs/GaSb superlattices:

- Absorption,
- Photoluminescence
- Minority carrier lifetime
- Lifetime temperature dependence

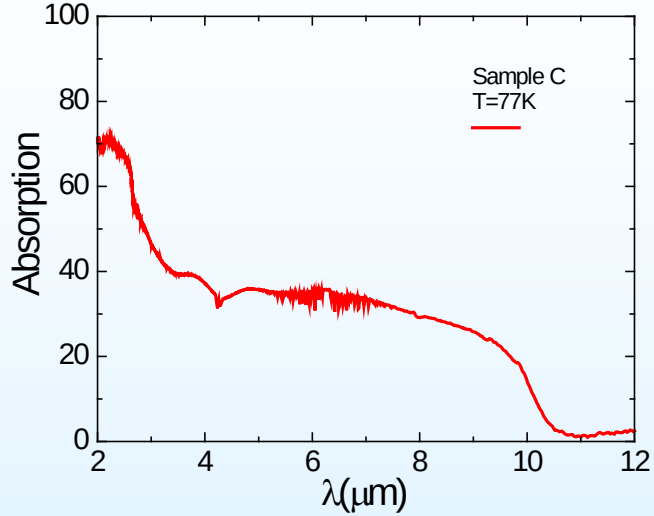

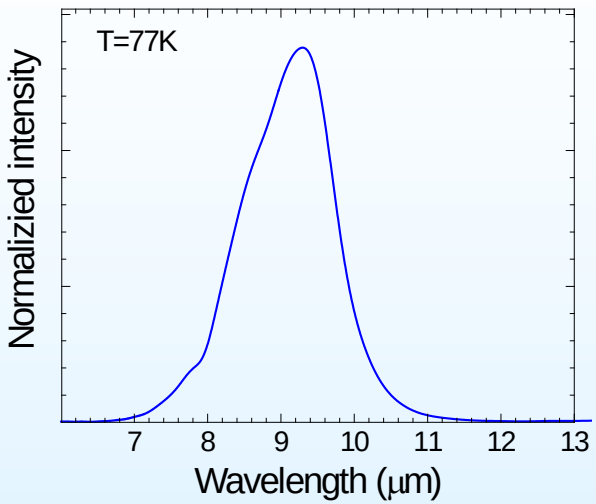

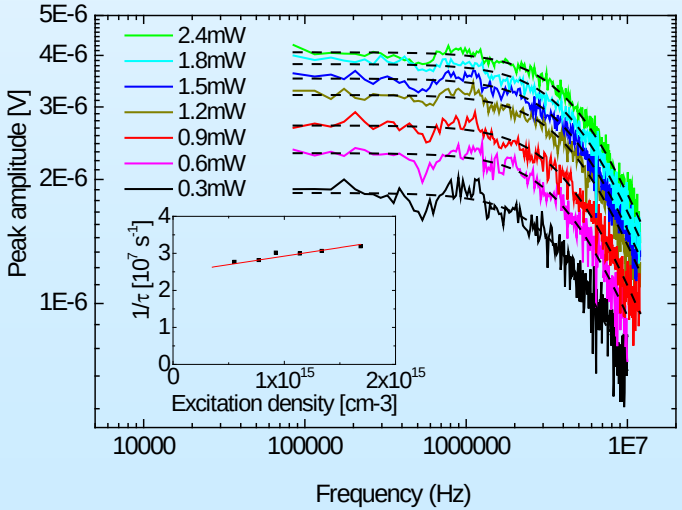

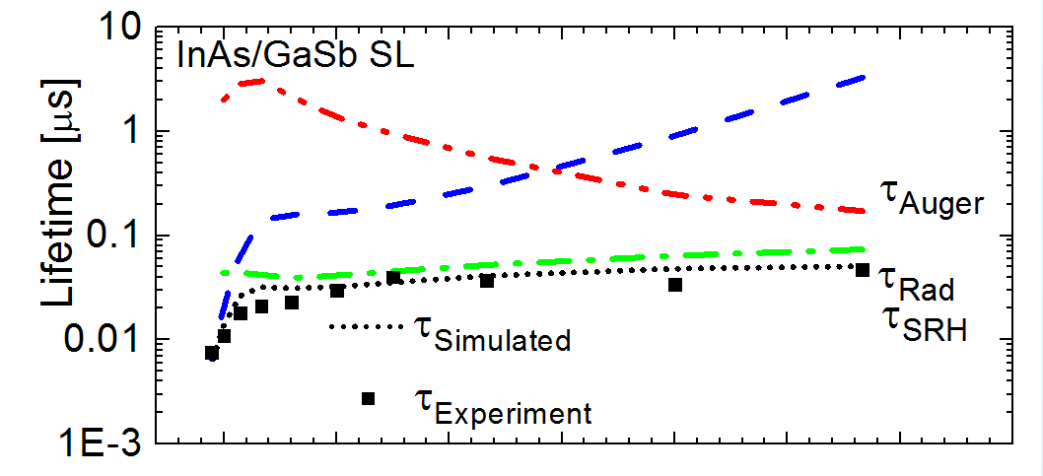

Hoglund et al. Appl. Phys. Lett. 103, 221908 (2013)

Outline

- Quantum Well Infrared Detectors
- Antimonide-based superlattice (SL) infrared photodetectors
- Barrier Infrared Detector (BIRD)
  - Complementary Barrier Infrared Detector (CBIRD)
  - **CBIRD focal plane array**
  - InAsSb barrier detectors
  - Quantum Dot Barrier Infrared detectors
- Ga-free InAs/InAsSb superlattices

Material Growth and Characterization

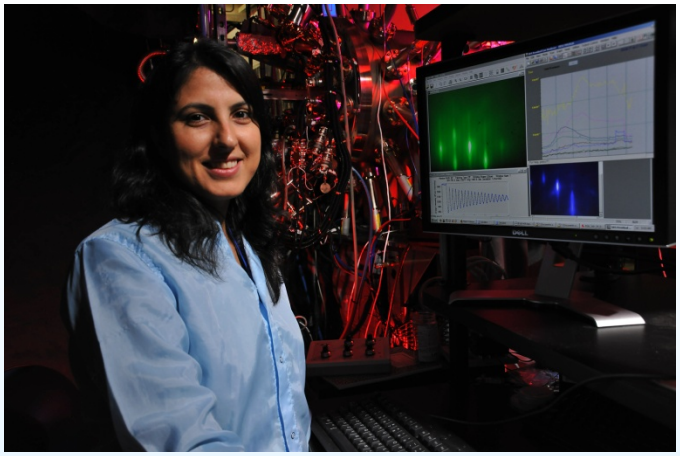

Gen-III MBE:
Superlattice growth

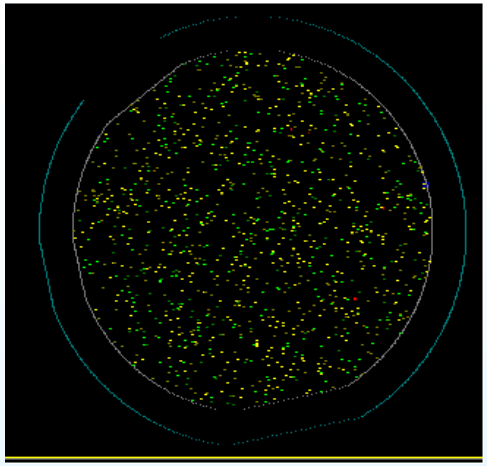

Surfscan: surface-quality
Particle count: 77.4/cm^2

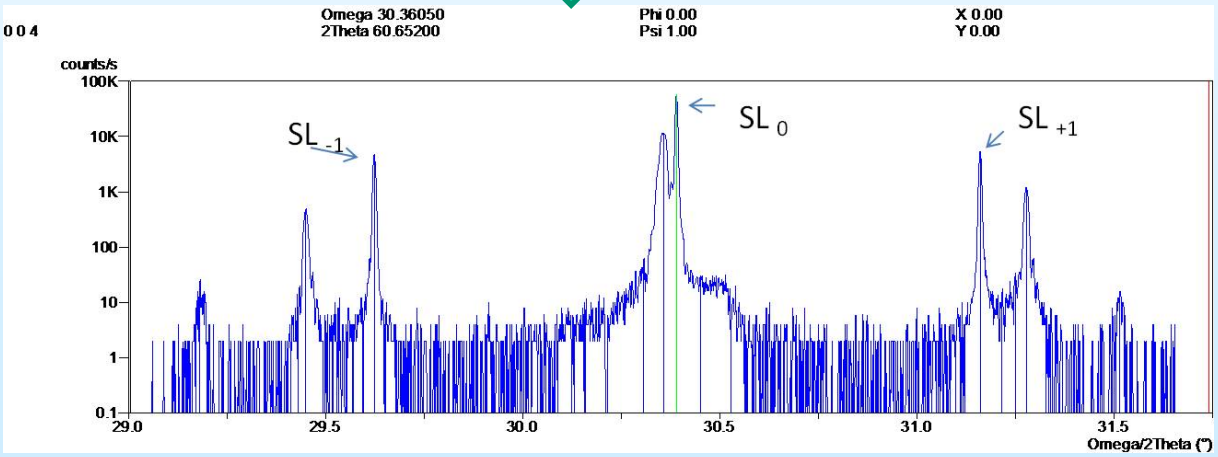

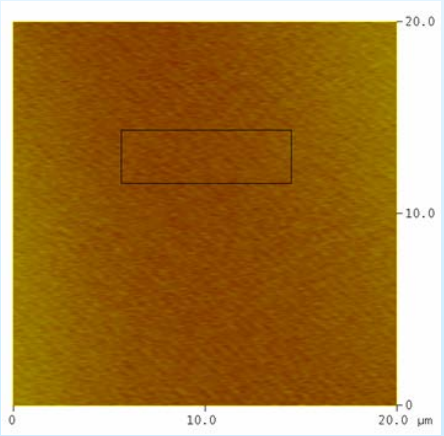

AFM: Surface morphology
20 µm x 20 µm scan
Defect free surface

XRD: Structural quality
Period: 66.4 Å
Average FWHM $SL_{+1,-1}$=21.67 arcsec

Combination Dry Etch

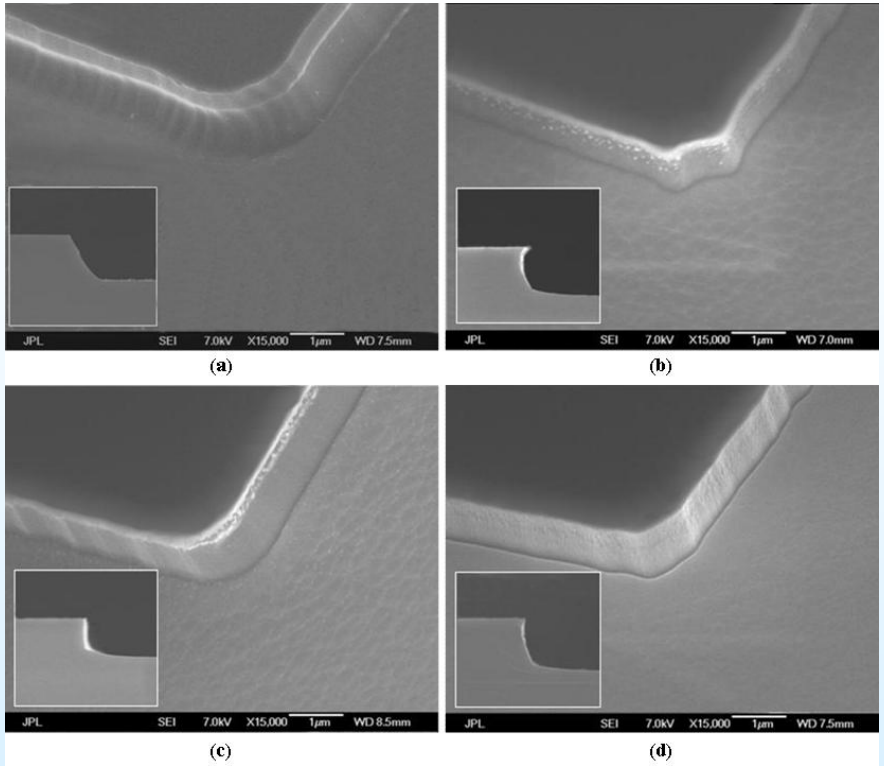

"Low dark current long-wave infrared InAs/GaSb superlattice detectors",

Jean Nguyen, A. Soibel, D. Z.-Y. Ting, C. J. Hill, M. C. Lee, and S. D. Gunapala,

Appl. Phy. Lett. **97**(5), 051108 (2010).

- $CH_4/H_2/BCl_3/Cl_2/Ar$ combination ICP dry etch technique
- Variable device size study shows lowest surface-to-bulk dark current ratio among several etch techniques
- Combination etch produced nearly vertical, smooth side walls
  - High fill factor favorable for FPA fabrication
  - Minimal dielectric mask erosion

CBIRD FPA

- ISC-0903 ROIC, 320x256 format, fully delineated
- T= 78K operating temperature, 300K background, f/2 optics
- Operability ~ 97% [$0.75*R_{MEAN} < R < 1.25*R_{MEAN}$]
- QE ~ 45% (4.5 – 9 µm)
- NEDT ~ 18.6 mK

CBIRD FPA

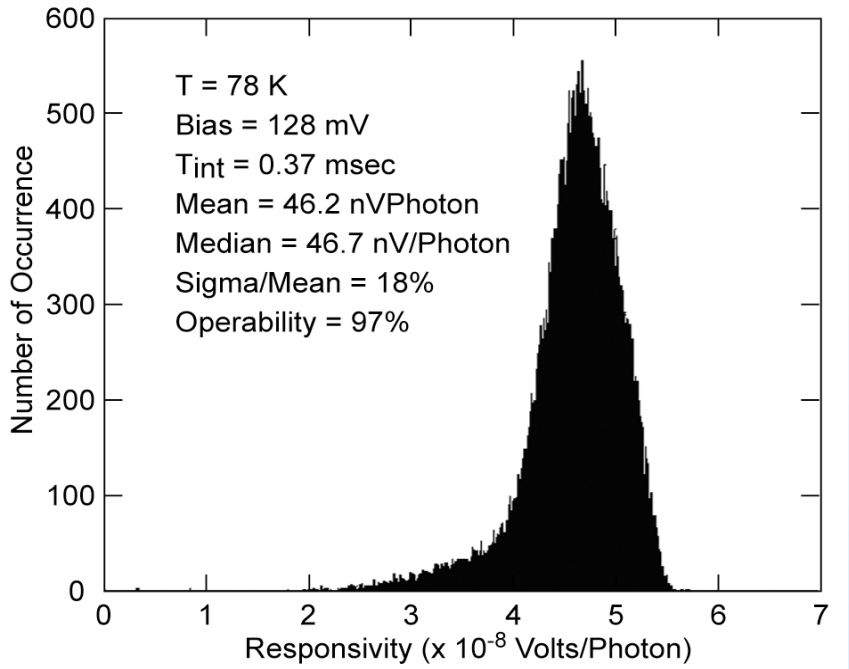

Responsivity histogram at 78 K operating temperature for an n-CBIRD FPA

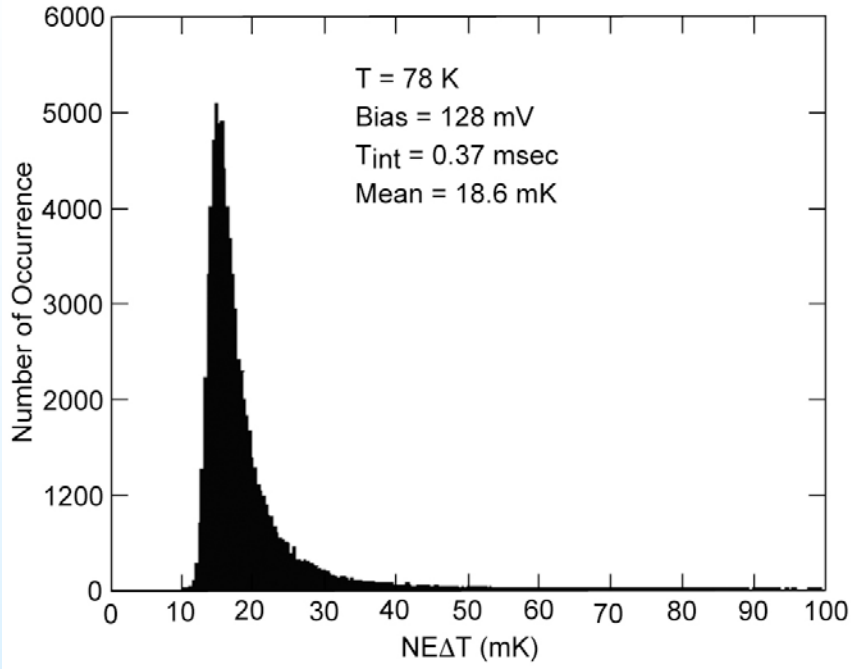

Measured n-CBIRD NEDT histogram operating at 78 K, bias of 128 mV and integration time of 370 msec. The mean NEDT is 18.6 mK

- Operability ~ 97% [$0.75*R_{MEAN} < R < 1.25*R_{MEAN}$]
- NEDT ~ 18.6 mK
- This value of NEDT implies good noise properties of detector and ROIC

Outline

- Quantum Well Infrared Detectors
- Antimonide-based superlattice (SL) infrared photodetectors
- Barrier Infrared Detector (BIRD)
  - Complementary Barrier Infrared Detector (CBIRD)
  - CBIRD focal plane array
  - **InAsSb barrier detector**
  - Quantum Dot Barrier Infrared detectors
- Ga-free InAs/InAsSb superlattices

Room temperature performance of Mid-Wavelength Infrared InAsSb nBn detectors

High operating temperature infrared detectors are important for many applications

- "Low-end" imaging where power consumption, size and cost are major constrains
- Chemical sensing such as in-situ tunable laser sensing

Thermal detectors operate at ambient temperature

- Significant progress in the recent years
- Slow
- Limited sensitivity

Quantum detectors which are typically based on semiconductor devices

- Better sensitivity and higher operational speed
- Typically require cryogenic cooling

Innovative detector architectures such as

- Barrier structures, in particular Barrier Infrared Detectors (BIRD) and nBn, devices
- Improvement in the performance GaSb-based alloys and superlattices

Can these novel detectors improve high temperature operation of Quantum detectors?

Barrier Infrared Detectors (BIRD) Design

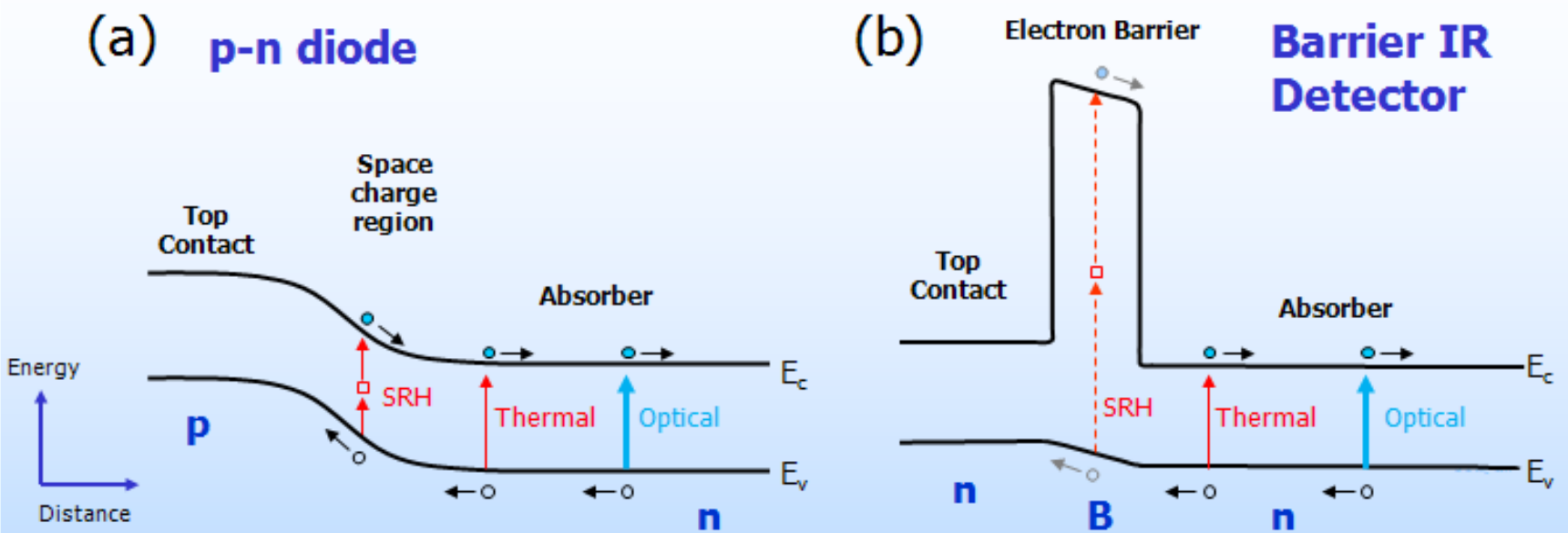

BIRD utilizes unipolar barriers:

- Block one carrier type, but allows un-impeded flow of the other

BIRD advantages

- Suppressed generation-recombination current
- Simplified fabrication process utilizing shallow etching into the barrier
- Elimination of surface leakage currents

Maimon, S., and G. W. Wicks (2006). nBn detector, an infrared detector with reduced dark current and higher operating temperature. Appl. Phys. Lett. 89, 151109
Klipstein, P. (2008). 'XBn' barrier photodetectors for high sensitivity and high operating temperature infrared sensors. Proc. SPIE 6940, 69402U-2.

Responsivity QE

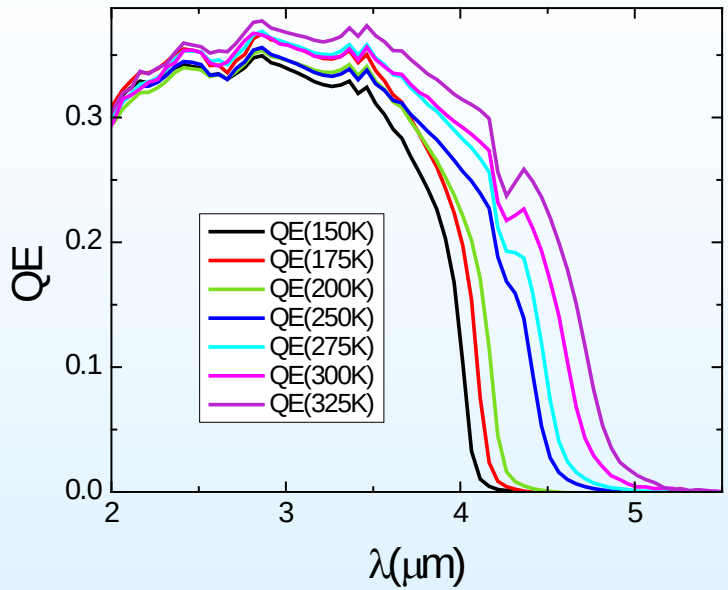

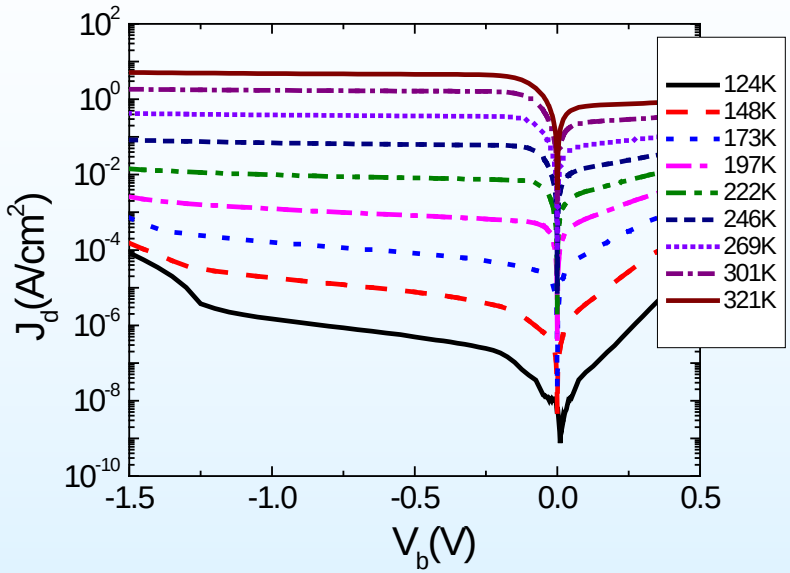

- Single pixel 200μm square devices were fabricated and tested.
- Front side illumination
- $QE_{max} \approx 0.35$
  - QE is for single pass
  - High substrate absorption

- Dark current density vs. applied bias in the temperature range from T = 124K to T = 321K.
- The dark current density at turn-on bias increases with temperature from
  - $j_d = 7\times10^{-7}$ A/cm^2 at T = 148K
  - $j_d = 6\times10^{-2}$ A/cm^2 at T = 246K
  - j_d =1.6 A/cm^2 at T = 300K

Detectivity

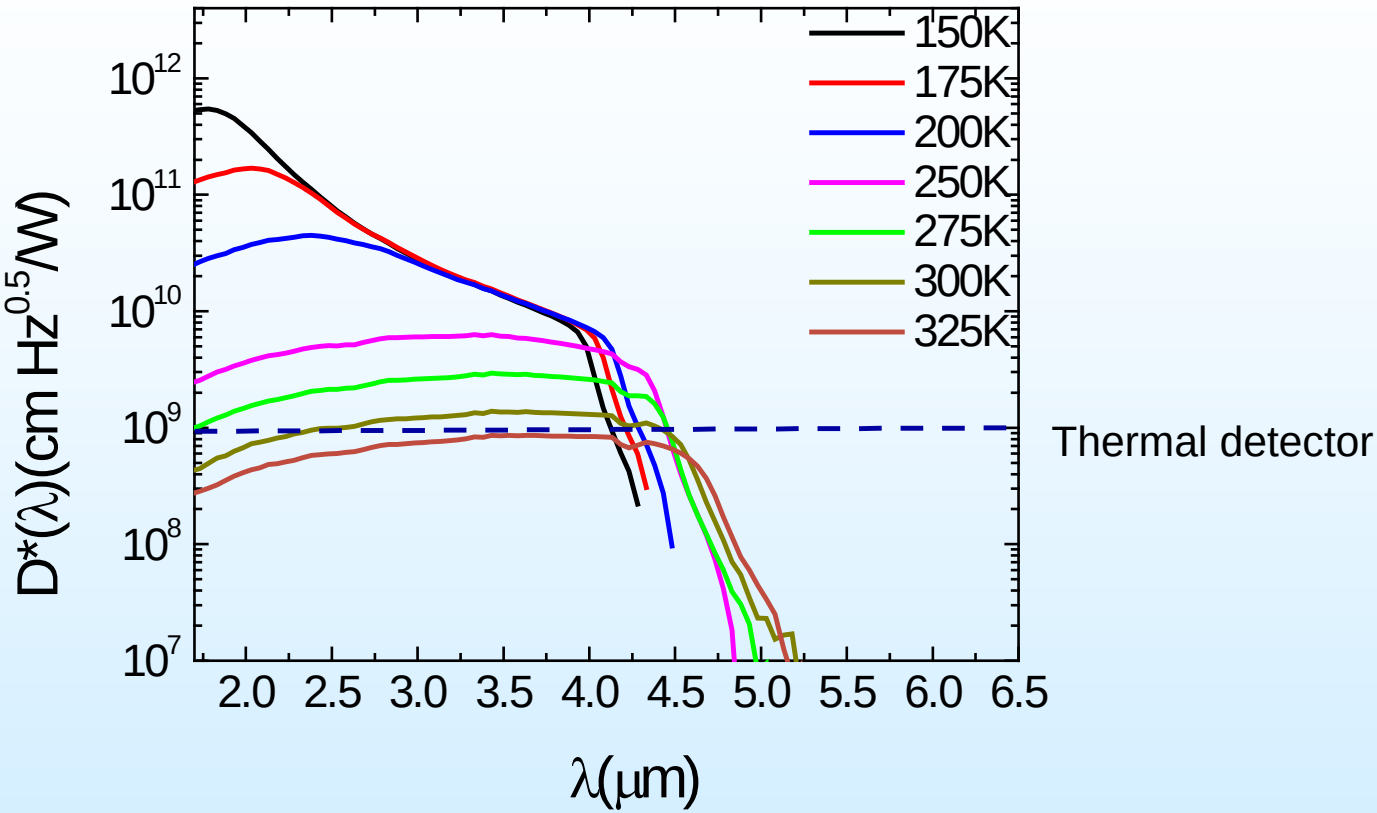

- Detectivity $D^*(\lambda)$ for background temperature of 300K and *f*/2 field of view
- $D^*(\lambda) = 1\text{x}10^9$ (cm $Hz^{0.5}$/W) at 300K

  Equivalent to the typical detectivity of thermal detectors
- $D^*(\lambda) = 5\text{x}10^9$ (cm $Hz^{0.5}$/W at 250K
- 3-5 times improvement in the detector detectivity can be achieved by increasing QE and by fabrication of microlens

Outline

- Quantum Well Infrared Detectors
- Antimonide-based superlattice (SL) infrared photodetectors
- Barrier Infrared Detector (BIRD)
  - Complementary Barrier Infrared Detector (CBIRD)
  - CBIRD focal plane array
  - InAsSb barrier detectors
  - **Quantum Dot Barrier Infrared detectors**
- Ga-free InAs/InAsSb superlattices

Standard nBn and QD-BIRD

Standard nBn:

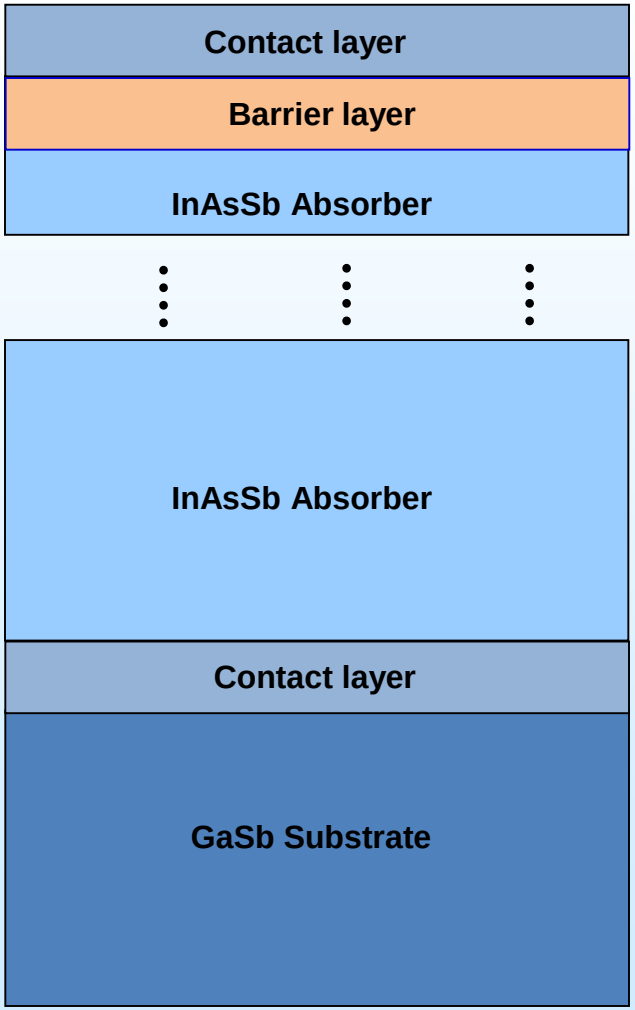

QD-BIRD:

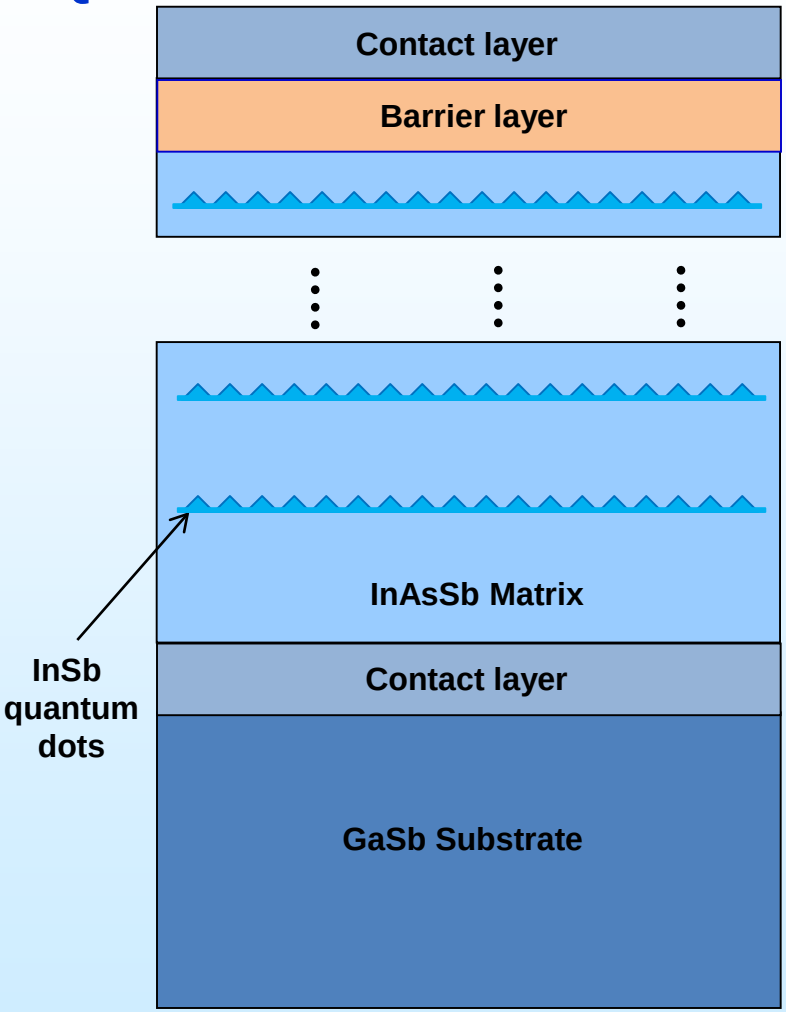

- QD-BIRD is based on a simple modification of the standard nBn
- Periodic insertion of InSb quantum dot layers

Type-II Broken-Gap Quantum Dots

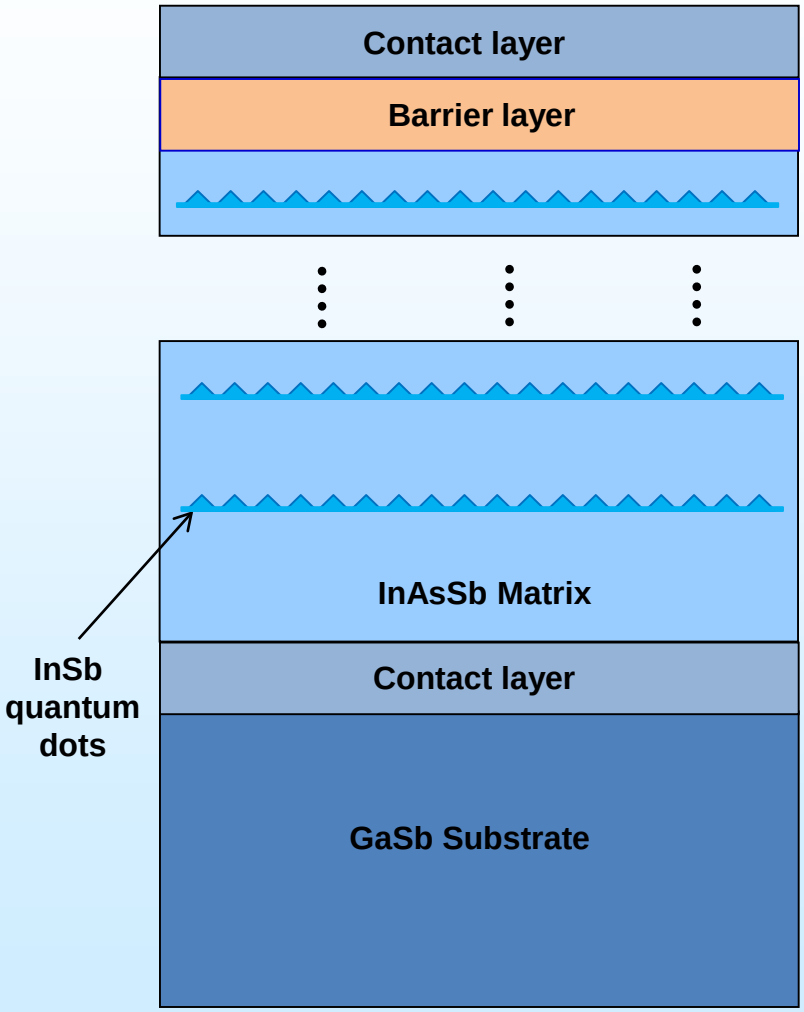

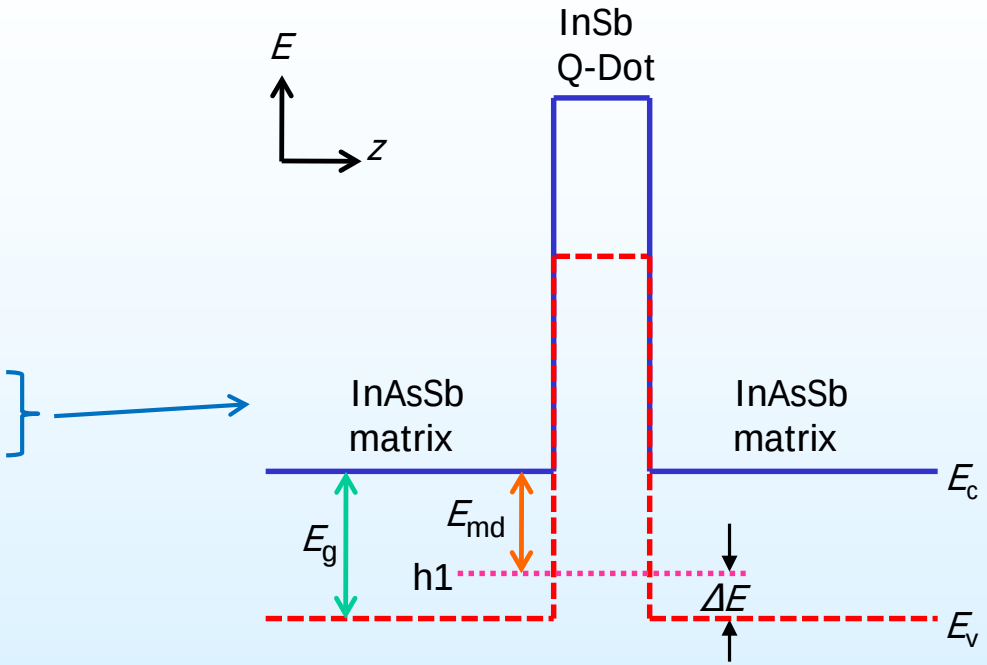

- Type-II broken-gap band alignment between InSb and InAsSb
- InSb QD conduction band state is in the continuum (unconfined)
- InSb QD valence band state can be confined in the gap of InAsSb matrix

Spectral Quantum Efficiency

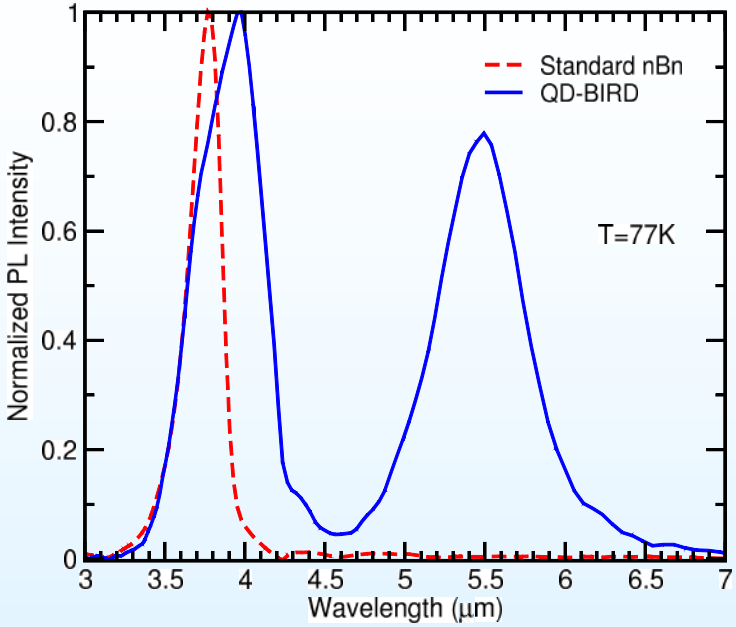

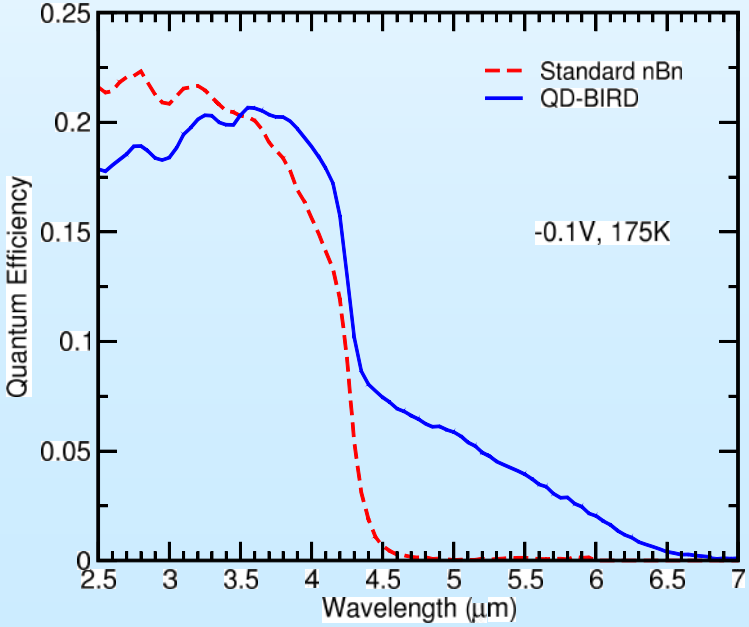

- Measured spectral response in top-illuminated configuration
  - No anti-reflection coating
  - GaSb substrate is transparent in MWIR
  - After initial pass, light could reflect from the bottom of substrate and back into the absorber region
  - Multi-pass response
- Corresponding <u>bimodal</u> behavior found for spectral response as in PL spectrum
- InAsSb matrix response similar to standard bulk InAsSb nBn
  - QE plateau
- Extended response out to ~6μm
  - Weaker than matrix response (unlike PL)
  - QE decreases with wavelength

Photo-Response and Dot Size Distribution

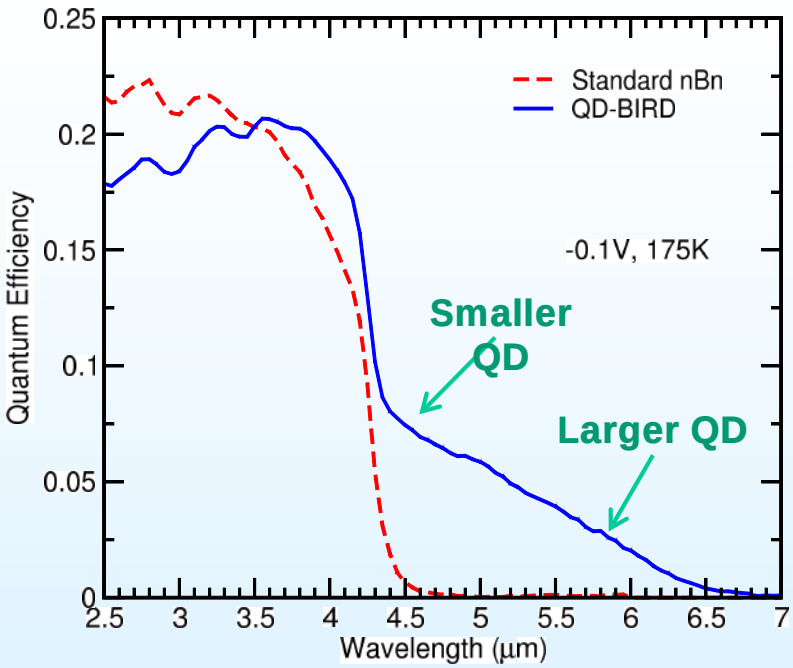

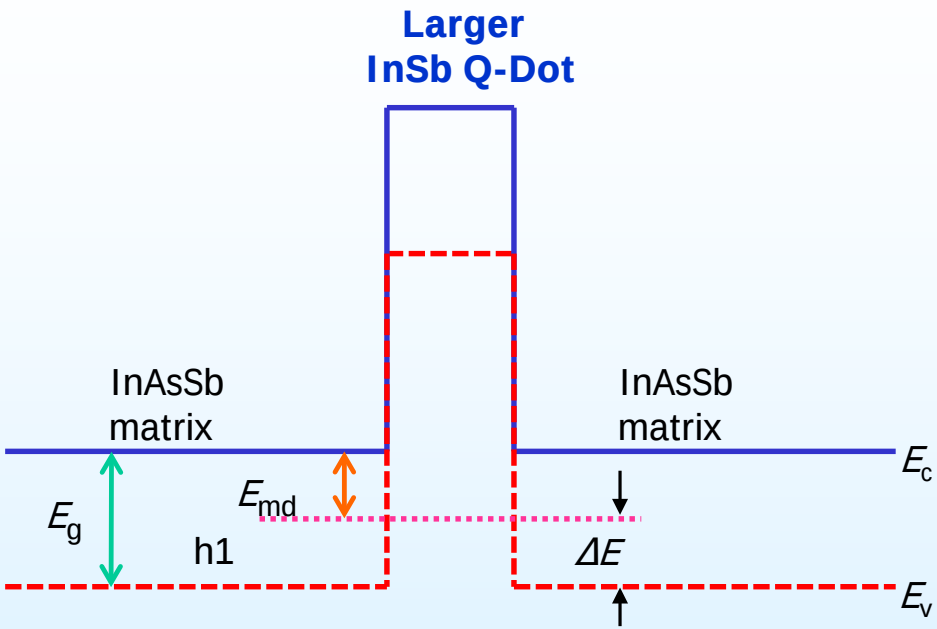

Corresponding <u>bimodal</u> behavior found for spectral response as in PL spectrum

Extended response out to ~6µm

Weaker than matrix response QE decreases with wavelength

- Large QDs have
  - smaller transition energy E_{md} , longer absorption wavelength
  - larger activation energy ΔE , lower hole escape probability, reduced photo-response

Dark Current Density and D*

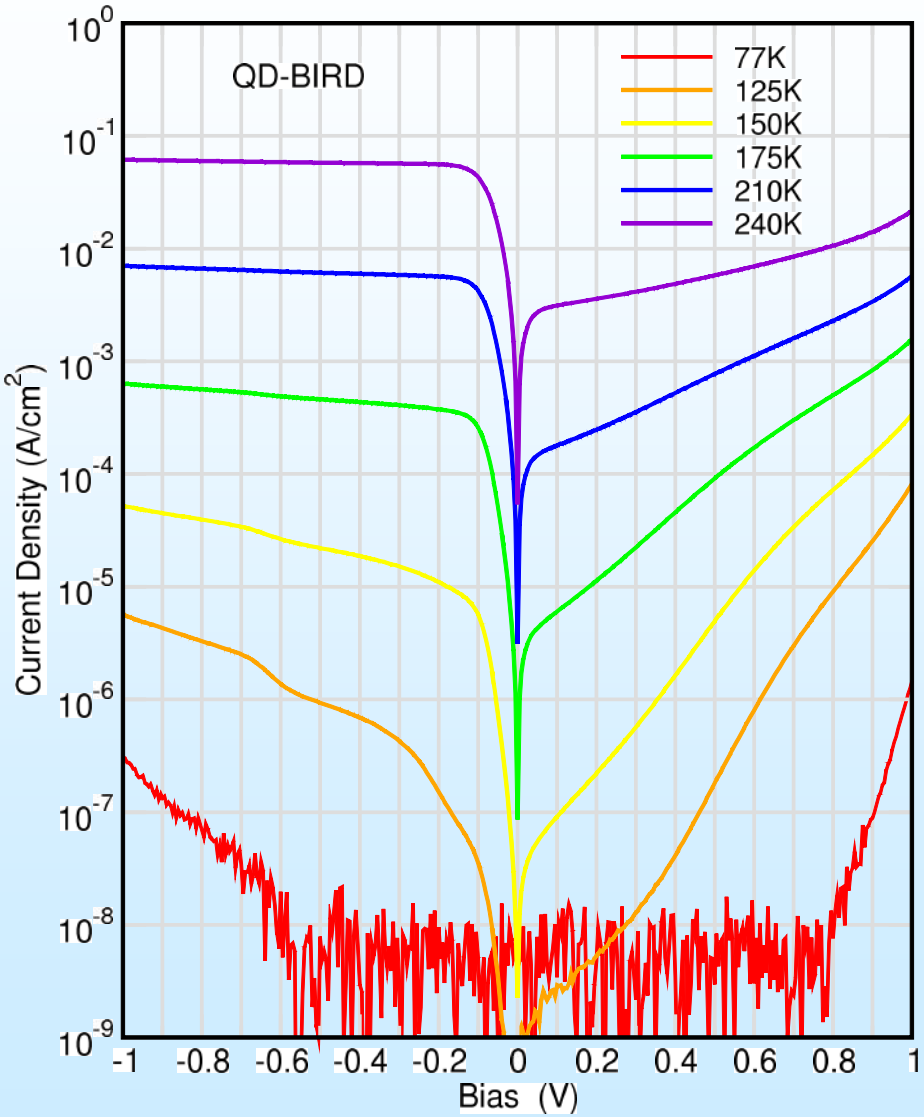

- Higher temperature reverse-bias I-V appears diffusion limited
- Lower temperature I-V shows exponential increase
  - Fowler-Nordheim barrier
- Reasonably low dark current
  - J(-0.2V, 175K)= 3.77×10^{-4} A/cm^2
  - J(-0.2V, 125K)= 1.52×10^{-7} A/cm^2
- Black-body D*
  - f/2, 300K background
  - Use integrated photo-response from 3 µm to 6 µm
  - D*(-0.2V, 175K)=1.07×10^{11} cm-Hz$^{1/2}$/W
    - Dark current limited
  - D*(-0.2V, 125K)=3.76×10^{12} cm-Hz$^{1/2}$/W
    - Background limited

Outline

- Quantum Well Infrared Detectors
- Antimonide-based superlattice (SL) infrared photodetectors
- Barrier Infrared Detector (BIRD)
  - Complementary Barrier Infrared Detector (CBIRD)
  - CBIRD focal plane array
  - InAsSb barrier detectors
  - Quantum Dot Barrier Infrared detectors
- **Ga-free InAs/InAsSb superlattices**

Lifetime in Ga-free InAs/InAsSb superlattice

Jet Propulsion Laboratory
California Institute of Technology

The **Ga-free InAs/InAsSb superlattices exhbit much longer minority carrier lifetime than InAs/GaSb (10μs vs <100ns))**

Auger, SRH and **radiative lifetime** all influence the minority carrier lifetime and the **shortest lifetime** will be dominating

$$\frac{1}{\tau} = \frac{1}{\tau_{SRH}} + \frac{1}{\tau_{R}} + \frac{1}{\tau_{Auger}}$$

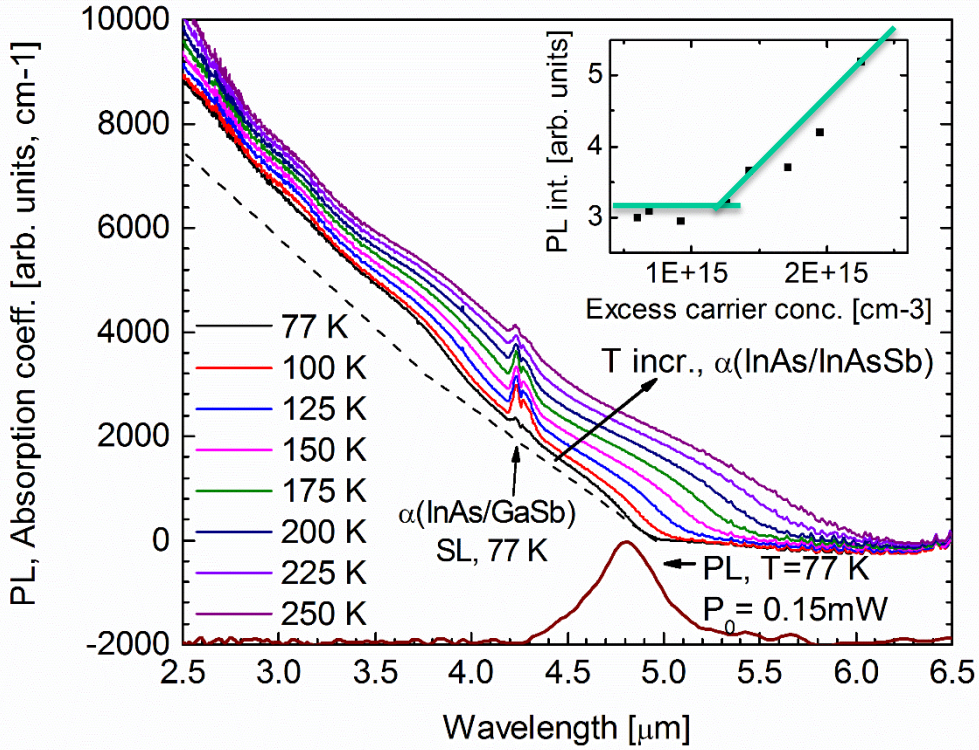

Sample studied:

- $InAs/InAs_{0.49}Sb_{0.51}$ superlattice
- Background doping ~1.5E15cm-3
- PL peak position ~4.8um
- Absorption coefficient ~1500cm^{-1} @4.5um

Influence of different recombination mechanisms on the lifetime

$$\tau_R = \frac{\phi}{Bn_0}$$

$$\tau_{SRH} = \frac{\tau_{n0}(p_0 + p_1) + \tau_{p0}(n_0 + n_1)}{(n_0 + p_0)}$$

$$\tau_{Auger} = \frac{2(n_i(T))^2 \tau_i}{(n_0(T) + p_0(T))\left[(n_0(T)) + \beta(T)(p_0(T))\right]}$$

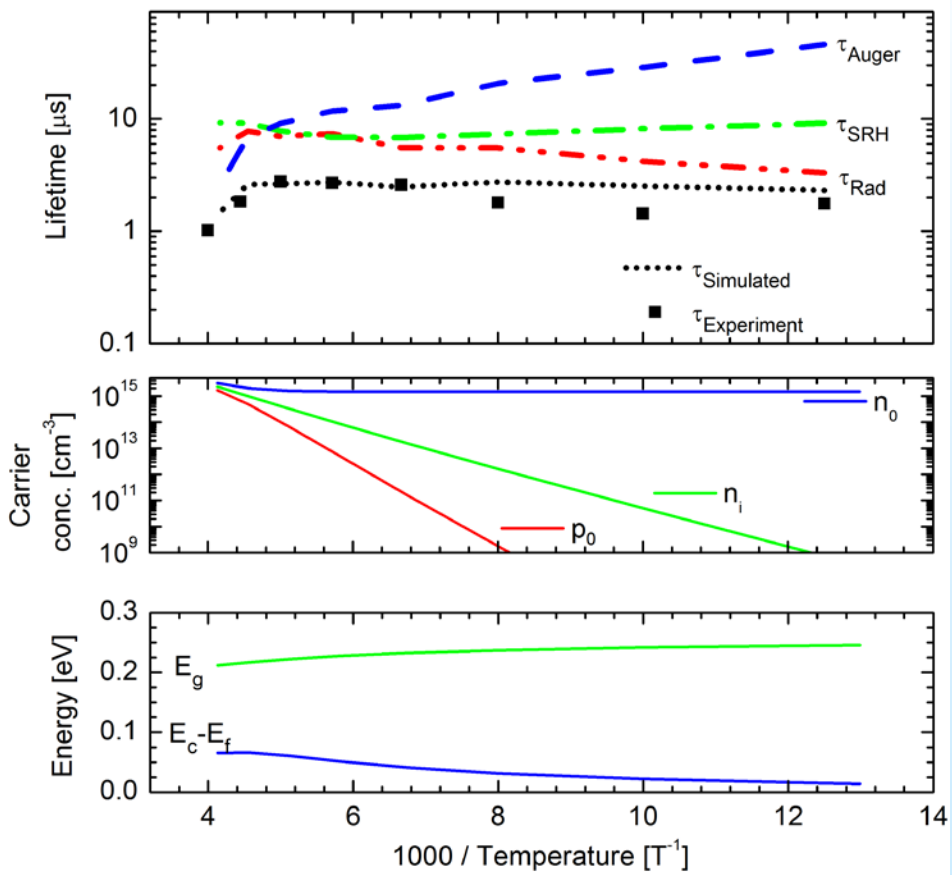

- Auger, SRH and Radiative lifetimes were calculated using parameters obtained from bandstructure calculations and experiments (m_c,m_v,$E_g(T)$,$E_f(T)$,$n_0(T)$,$p_0(T)$,$\alpha(T)$…)

→ **At low temperatures the radiative lifetime is dominating**

→ **SRH lifetime ~ 10us**

→ **Background doping is crucial for the lifetime.**

Summary

Barrier infrared detectors based on III-V compound semiconductors offer a breakthrough solution for the realization of low cost, high performance mid- and long-wavelength infrared imagers